# Analysis of Microwave Characteristics of 2D-Material based Nanocomposites

By

**Mobashir Hanif**

00000329927

Supervisor

**Dr. Fouzia Perveen Malik**

---

In the fulfillment of the prerequisites for *Master of Science* degree in

Computational Science & Engineering

Computational Sciences Department

School of Interdisciplinary Engineering and Sciences (SINES)

National University of Sciences and Technology (NUST)

Islamabad, Pakistan

**April 2023**

*DEDICATION*

*I dedicate this dissertation to my Parents,*
*for their endless love, support and encouragement especially my late father Muhammad Hanif*

# Declaration

I, *Mobashir Hanif*, declare that this thesis titled "Analysis of microwave absorption and characteristics of polymer-based nanocomposites" and the work presented in it are my own and has been generated by me as a result of my own original research.

I confirm that:

1. This work was done wholly or mainly while in candidature for a Master of Science degree at NUST.
2. Where any part of this thesis has previously been submitted for a degree or another qualification at NUST or any other institution, this has been clearly stated.
3. Where I have consulted the published work of others, this is always clearly attributed.
4. Where I have quoted from the work of others, the source is always given. With the exception of such quotations, this thesis is entirely my own work.
5. I have acknowledged all main sources of help.
6. Where the thesis is based on work done by myself jointly with others, I have made clear exactly what was done by others and what I have contributed myself.

_____

Mobashir Hanif

00000329927

# Copyright Notice

# Acknowledgments

I would first like to thank my thesis supervisor Dr. Fouzia Perveen Malik of the School of Interdisciplinary Engineering and Sciences, NUST. Whenever I encountered difficulties in development or thesis writing, his office door was always open to provide assistance. And consistently encouraged me to take ownership of this thesis, he also guided me in the right direction whenever he felt it was necessary. I am particularly grateful to the principal of the School of Interdisciplinary Engineering & Science, NUST, whose timely support served as a constant source of motivation for this project. Additionally, I extend my gratitude to the other members of the GEC, namely Dr. Muhammad Tariq Saeed and Dr. Manzar Sohail, for their unwavering support and assistance throughout the research phase.

I would like to express my gratitude to the Management of SINES, NUST, for their exceptional support and assistance in organizing presentations and demos for this research project. Their unwavering support was invaluable throughout the research phase. I am also thankful to Azmat Ullah and my fellow researchers in the Research Group for their valuable contributions and assistance during the research phase.

## Table of Contents

# List of Abbreviations and Symbols

**EMR** Electromagnetic Radiation

**RFID** Radio Frequency Identification

**MAMs** Microwave Absorbing Materials

**PANI** Polyaniline

**SWCNTS** Single Wall Carbon Nanotubes

**MWCNTs** Multi-Wall Carbon Nanotubes

**MOF** Metal Organic Framework

**PU** Polyurethane

**$MoSe_2$** Molybdenum Diselenide

**$MoS_2$** Molybdenum Disulfide

**RL** Reflection Loss

**ELF** Extra Low Frequency

**SLF** Super Low Frequency

**CST MWS** Computer Simulation Technology Microwave Studio

# List of Tables

## List of Figures

## List of Equations

## Abstract

Microwave absorptive materials (MAMs) are gaining significant attention due to their demand in various fields such as aerospace, electronics, medical, and defense. These materials shield microwaves by absorbing or reflecting the radiation. In this study, we determine the electromagnetic parameters of materials which is based on the principle of the interaction between the electromagnetic field and the electromagnetic medium. For their microwave absorption behavior, two composite materials were designed and tested *i.e.,* $MoSe_2$/Alumina and $MoSe_2$/$MoS_2$. To analyze the effective permittivity of nanomaterial samples Maxwell Garnett effective medium theory was used. For extraction of S-Parameters in the X and Ku band range (8-18 GHz), models of these composite materials were generated. The Reflection Loss, total Shielding, and percentage absorption were calculated for these samples. In X-band range, 4mm thick sample of 0.4% MoSe2/Alumina composite showed the maximum reflection loss value of -57.12dB. The $MoSe_2$/Alumina composite exhibited higher values of real part of effective permittivity. This can be the reason for enhanced microwave absorptive property of this composite. On the other hand, for $MoSe_2$/$MoS_2$ composite in X-band only a maximum RL value of -0.5dB was observed. Small thickness of the composite can be responsible for the low reflection loss. However, in Ku band, the MoSe2/MoS2 composite with a 3mm thickness demonstrated the highest value of reflection Loss, of -51.90dB. It was found that both MoSe2 and MoS2 use the reflection phenomenon for microwave shielding. The achieved microwave absorbing properties of the MoSe2/MoS2 nanocomposites suggest promising applications in high-performance microwave absorbers. By incorporating 2D transition metal dichalcogenides (TMDs) composites into our work, we can explore new applications which was not feasible or optimized with polymer-based nanocomposites such as electronics and defense industry. By utilizing TMDs composites, we can potentially enhance performance, increase efficiency, or enable entirely new functionalities in these application areas.


**Keywords:** *Microwave Absorbing Materials, X-band, Ku-band, Maxwell Garnett effective medium theory, S-parameters*

# Chapter 1: Introduction

In the electromagnetic radiation, it propagates across the range from extremely brief gamma rays (wavelength 10-12m) to x-rays, ultraviolet rays, visible light waves, and even longer Infrared waves. These longer waves encompass microwave and radio waves, which can extend over vast distances, comparable to the expanse of a mountain range. This spectrum serves as the fundamental basis for information in the modern world. Devices such as radios, remote controls, text messaging, televisions, microwave ovens, and even certain medical instruments like x-rays all rely on waves within the electromagnetic spectrum. Electromagnetic waves bear resemblance to ocean waves, as they both carry energy and transmit it. Charged particles generate electromagnetic waves, possessing electrical and magnetic properties, which travel through the vacuum of space at a constant speed of light. These waves exhibit crests and troughs like ocean waves, with the distance between two crests known as the wavelength. Some waves have long wavelengths measured in meters. Frequency refers to the number of crests passing through a given point per second. Radio waves, with their long wavelengths, have the lowest frequency and carry less energy. Increasing energy raises the frequency and shortens the wavelength of waves. Gamma rays, the shortest and highest energy waves, exist in the spectrum. While watching TV, various waves reach our eyes, including visible light waves, radio waves from nearby stations, microwaves from cell phones transmitting calls and text messages, as well as waves from Wi-Fi and GPS. This results in a chaotic mixture of waves. Tuning a radio to a specific station resembles our eyes' ability to detect energy within the electromagnetic spectrum, ranging from 400nm to 700nm. Objects appear colourful because electromagnetic waves react with their molecular structure. Some of the wavelengths in the visible region spectrum are reflected, while the others are absorbed. The green colour of a leaf, for example, is due to EM waves interacting with chlorophyll molecules, with wavelengths between 492nm and 577nm being reflected, creating the perception of green. Objects emit, reflect, and absorb EM radiation differently based on their composition. By studying unique information contained in waves across the electromagnetic spectrum, we continuously learn more about our world and the universe. Based on these findings, specifically designed composite materials can be highly useful in different kinds of fields, such as defense industry and electronic gadgets, due to their exceptional microwave absorption properties. Computational investigations indicate the potential effectiveness of these designed composites as coating materials, although experimental testing is necessary to validate the computational findings.

## 1.1 Background

Electromagnetic radiations are important in our daily life and this has been the focus of interest for many scientist as well as the researchers. JC Maxwell in 1965 proposed light as the electromagnetic phenomenon and gives the correspondence to the electrical and magnetic area the current with their charges help of some mathematical models. After that Heinrich Hertz in 1887 proved the presence of radiations via his experiment. Electromagnetic radiations are consisting of series of crust and trough of oscillating electric and magnetic field, for which this energy can travel in space without any supportive medium. Electromagnetic spectrum spread from short gamma rays to x-rays, ultraviolet-rays, visible light waves, even longer infrared waves, microwave to radio waves which longer waves. In electromagnetic waves microwaves are the crucial part because they are used in telecommunication Technology, microwave absorbing materials, etc. Long-time exposure to microwave radiation can cause body tissues burn.

So, along with finding new applications of microwave radiations, researchers are also working to find techniques or materials that can minimize the harmful effects of microwave radiations. Microwave absorptive materials (MAMs) are point of special interest to material scientists in this regard. [1-2].

## 1.2 Microwave Radiations

Microwaves fall between radio waves and infrared, which is ranging from 30cm down to 1mm and frequency is ranging from 300MHz to 300GHz. Different wavelength of microwave, grouped into bands which provide different information to the scientists. According to Institute of Electrical and Electronics Engineering (IEEE) different ranges or bands are given to microwave frequency range. Microwaves of moderate length can penetrate through smoke, snow, dust particles, clouds, and rain. And utilization of these ranges has great important telecommunication. [3]

## 1.3 Subranges of Microwave Radiations

ELF is used specifically for pipeline transportation; this frequency range is employed for underwater communication. SLF is used in the power grid and for communications between submarines. ULF used for military and mining purposes. This frequency spectrum penetrates mud and rock and is utilised for geophysics, navigation, and wireless heart monitoring. VLF This frequency spectrum penetrates mud and rock and is utilised for geophysics, navigation, and wireless monitoring. RFID, amateur radio, and navigation also use LF. MF frequency band encompasses AM broadcasting, coast-

to-sea communication, etc. HF is used in aviation and weather applications. VHF is useful in analogue television and medical equipment. UHF is important for latest wireless communications. SHF is used for 5GHz Wi-Fi, mobile networks and microwave equipment. EHF is useful for microwave sensing and relays. THF replaces X-rays in Terahertz imaging.

Table 1.1: Microwave Frequency bands

| Sr. No | Frequency Bands | Frequency |
|---|---|---|
| 1 | Extremely low frequency (ELF) | 3 Hz-30 Hz |
| 2 | Super low frequency (SLF) | 30 Hz-300 Hz |
| 3 | Ultra-low frequency (ULF) | 300 Hz-3 kHz |
| 4 | Very low frequency (VLF) | 3–30 kHz |
| 5 | Low frequency (LF) | 30–300 kHz |
| 6 | Medium frequency (MF) | 300–3,000 kHz |
| 7 | High frequency (HF) | 3–30 MHz |
| 8 | Very high frequency (VHF) | 30–300 MHz |
| 9 | Ultra-high frequency (UHF) | 300–3,000 MHz |
| 10 | Super high frequency (SHF) | 3–30 GHz |
| 11 | Extremely high frequency (EHF) | 30–300 GHz |
| 12 | Terahertz high frequency (THF) | 300–3,000 GHz |

### 1.4 Bands of Frequency

The table below lists some of the uses for microwave frequency bands as suggested by the IEEE. This region has great importance as it is used for global positioning system, forest mapping, maps and times series of Arctic Sea, etc.

Table 1.2: Microwave Frequency bands and Their Applications

| Sr.No | Band Name | Frequency Region | Wavelength Region | Applications |
|---|---|---|---|---|
| 1 | L_Band | 1-2 GHz | 5-30.01 cm | Cell Phones, Positioning |
| 2 | S_Band | 2-4 GHz | 7.60-15 cm | Microwave ovens, Mobile Phones |
| 3 | C_Band | 4-8 GHz | 3.75-7.5 cm | Telecommunication |
| 4 | X_Band | 8-12 GHz | 25-37.5 mm | Radar, Satellite Communication |
| 5 | Ku_Band | 12-18 GHz | 16.7-25 mm | Molecular Rotational Spectroscopy |
| 6 | K_Band | 18.1-26 GHz | 11.2-16.6 mm | Radar Communication |
| 7 | Ka_Band | 26.5-34 GHz | 5.1-11.3 mm | Satellite Communication |
| 8 | Q_Band | 33-50 GHz | 6.01-9.0mm | Satellite Communication |
| 9 | U_Band | 40-60 GHz | 5.00-7.5mm | Satellite Communication |
| 10 | V_Band | 50-75 GHz | 4.10-6.00mm | Research area |
| 11 | W_Band | 75.5-110.5 GHz | 2.7-4.00mm | Millimetre Wave Radar Research |
| 12 | F_Band | 90-140 GHz | 2.1-3.3mm | Satellite television broad casting |
| 13 | D_Band | 110-170 GHz | 1.8-2.7mm | Millimetre Wave Scanner |

### 1.5 X_band Region

Fundamentally, it is used by military for microwave absorbing applications including constant waves, signal polarization and phase arrays. Civil, military, and government agencies employ X-band radar for weather recording, examine defence, automobile speed recording for the implementations of rule enforcement.

### 1.6 Ku_band Region

Ku-Band have prime importance in satellite communication. PAKSAT-1 gives Pakistan, Africa, and the Middle East high-quality Ku-band satellite communications. [4] Ku-band transponders give full features to study High-power payloads in geostationary orbit. [5]

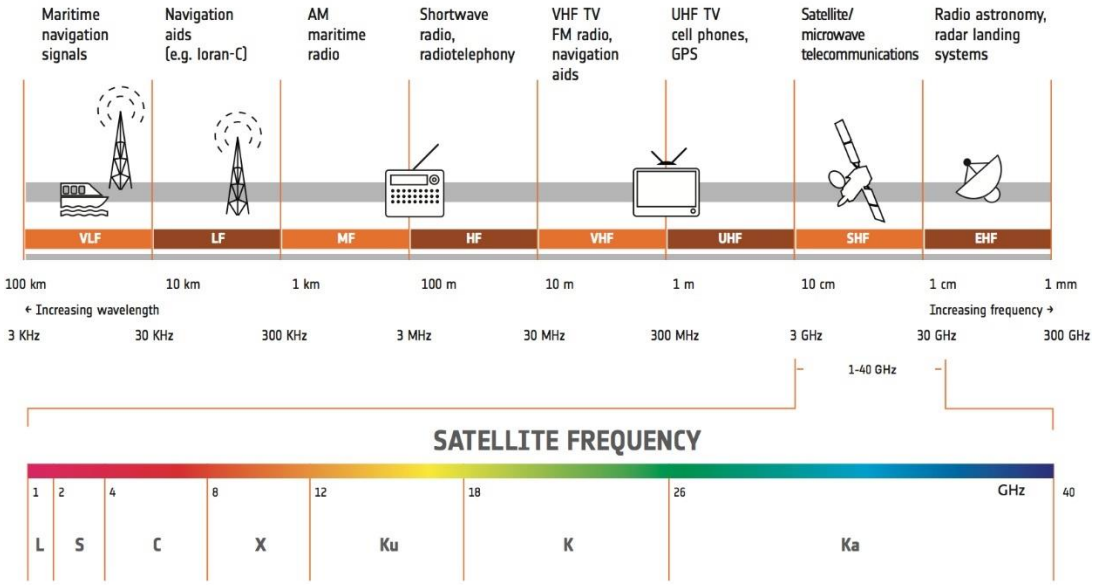


Figure 1.1: Frequency Ranges with Areas of Applications

### 1.7 Technical Knowledge of Microwave

With the progress in electronics and software technologies, there has been a significant rise in the level of electromagnetic (EM) radiation that people are being subjected to. Ionized and non-ionized radiation make up most of the electromagnetic radiation. Ionizing radiation is a high frequency electromagnetic pulse (greater than 1014 Hz) that has the power to ionise atomic bonds in cellular equipment. For example, X-ray and gamma rays, etc. The energy of non-ionizing electromagnetic radiation is insufficient to break atomic bonds.

Other useful impacts of microwave technology are in electronics, navigation, radar systems, food industry, spectroscopy, research applications, etc [5]

Microwaves are an important part of electromagnetic spectra due to their many uses. We can't ignore the risks of microwave radiation, though.

*Interference:* When almost every electronic gadget around us is utilizing electromagnetic radiations there is always a chance of interference among the devices. For example, use of microwave oven in the vicinity of a Wi-Fi can interfere with its signals, and result in weakening the Wi-Fi signals in the phone or the laptop. In hospitals, where different life saving procedures and instrument uses electromagnetic radiations possibility of EMR interference is always there, which can lead to some life-threatening situation for a patient. [6]

*Issues related to our health:* We ourselves are always exposed to some form of electromagnetic radiations, of which microwave radiation is a prominent part. This can lead to various health problems. These effects are of two types: Thermal – high frequency, high power associated with heat; Non-Thermal – Low frequency, low power. Various papers discuss the impact of continuous exposure of microwave radiations to central nervous system of human being – causing many long term and short-term brain problems. Many other medical conditions like reproductive, endocrine, cognitive and even cancer have been reported in various studies. [7-11]

Pollution from Electromagnetic Radiations: Microwave technology, which is utilised in virtually all communication equipment such as Wi-Fi, mobile phones, Wi-Fi transmissions, radar signals, etc., is the main factor contributing to this pollution.

All these problems associated with extensive use of microwave technology make it clear that we must develop the materials that can act as a shield from these harmful radiations from electromagnetic spectrum. [12-14]

## 1.8 Microwave Absorbing Materials:

Due to its value in stealth technology and ability to effectively reduce electromagnetic pollution, microwave absorbent materials (MAMs) are at the centre of study in the field of materials. By transforming microwave radiation into heat, they can dissipate it. Given that, as was previously mentioned, practically every aspect of life today employs microwave technology, there is a wide range material, from inorganic to organic origin and hybrid. MAMs reflect or absorb microwave radiation to shelter it. Material scientists are developing affordable, robust, and microwave-shielding materials.

## 1.9 Types of MAMS:

Based on chemical properties MAMs are classify into the following broad categories:

- Organic MAMs.
- Inorganic MAMs.
- Mixed/Hybrid MAMs.

### i) Organic Microwave absorbing materials (MAMs):

Conducting The electrical characteristics of polymers make them the potential new absorbing materials. These polymers include, among others, PANI (polyaniline), polypyrrole, and Poly azomethine esters, etc

### ii) Inorganic Microwave absorbing materials (MAMs):

Most commonly commercially accessible inorganic microwave absorption materials are numerous. And most important ones are.

- Iron- based ferrite absorbing materials, fibres of polycrystalline, carbonyl iron are some of them.
- Carbon based absorbing materials, for example SWCNTs (single carbon nanotubes), MWCNTs, Graphdiyne, Graphene, Nano Carbon, etc.
- Ceramic based absorbing materials, for example Alumina, Silicate Ceramics, Glass ceramics, Carbide based ceramics, etc.

### iii) Mixed/Hybrid Microwave absorbing materials (MAMs):

To produce the desired qualities, these multifunctional materials combine organic and inorganic components. These are either a mixture of the two materials (organic/inorganic) created by physical means, such as nano composites, or they are chemically combined to form a single structure called a metal organic framework (MOF). When mixed with polymers as a filler, MOFs can also be employed as polymer nanocomposites.

## 1.10 Nanocomposites:

Nano composites are multicomponent, multiphase non-gaseous hybrid materials, in which at least one of the phases has with least one dimension less than that of 100 nm. These materials can be formed by conducting organic polymers used as matrix and the inorganic nano particles such as graphite, gold, carbon nano tubes, graphene, tungsten sulfide etc. dispersed in the matrix as a filler. The small quantity of nanofiller enhance various properties of polymers tremendously, including microwave absorption properties. Nanocomposites can be made without polymer as matrix in them as well. [15,16]

### Types of Nanocomposites

Nanocomposites can be classified into different groups based on their nanoscale size, their dispersion medium, or the way the nanofiller in the matrix reacts chemically.

### i) Type based on nano scale dimensions:

The following categories of nano composites exist depending on how many nanoscales dimensions the nano fillers have:

**a)** Zero-dimension (0D) nanocomposites – Spherical nanomaterials, also known as 0D nanomaterials, are characterized by their ultra-small size as none of their dimensions exceed 100 nm. Due to this feature, they display a phenomenon known as quantum confinement and exhibit exceptional physical and chemical properties, which makes them one of the most extensively used types of nanomaterials. Examples are nanoparticles, spheres, clusters, quantum dots, clathrates, *etc.*

**b)** One-dimensional or (1D) nanocomposites – Nanomaterials with dimensions ranging from 1 to 100 nm in two directions, displaying high aspect ratios and diverse morphologies, are

classified as 1D nanostructures. This category of nanomaterials exhibits enhanced compatibility with biological structures.

**c)** Two dimensional or (2D) nanocomposites – 2D nanomaterials refer to materials where two dimensions are outside the nanoscale range, typically exceeding 100 nm. These kinds of nanomaterials gives unique physical, chemical, and mechanical parameters that are different from their bulk part due to their reduced dimensions. Examples are thin films, graphene, dimethyl dichalcogenides, graphdiyne, etc.

**d)** Three dimensional or (3D) nanocomposites – Nanostructures combine various nanoscale features in a single structure, providing a superior electroactive surface area. Examples are nanoparticles (bulk materials).

**ii) Classification based on dispersion medium:**

The nanocomposites are divided into two major parts based on the dispersed matrix and dispersion phase materials:

**a) Polymer based nanocomposites**

These contain a polymer matrix with filler material scattered throughout. It is a crucial subfield of nanocomposites because even a tiny amount of nanomaterial improves the mechanical, thermal, and absorptive characteristics of the bulk polymer matrix medium. These can also be divided into

**i.** Composites made of ceramic and polymers

**ii.** Nanocomposites of inorganic and organic polymers

**iii.** Hybrid inorganic/organic nanocomposites

**iv.** Layered silicate nanocomposites made of polymers

**b) Non-polymer-based nanocomposites**

The nanocomposites that are not being used polymer as a matrix are said to be non-polymer nanocomposites. These could also be categorised as metal-based, ceramic based and ceramic-ceramic based nanocomposites.

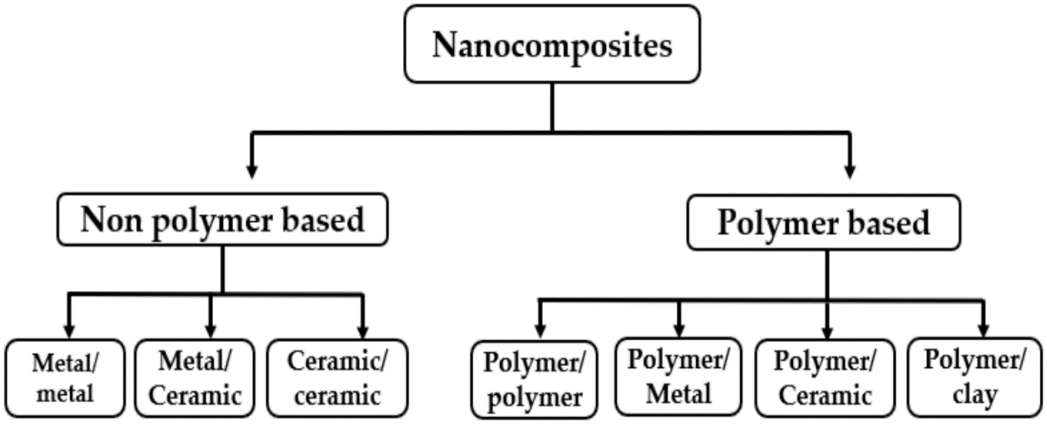


Fig 1.2. Classification of nanocomposites [17]

### iii) Classification based on nanofiller:

Nanocomposites can be divided into different categories according to the chemical make-up of the filler. A few key ones are:

**Carbon based nano composites:**

These composites have revolutionized the whole stock of already present microwave absorptive materials. Only small quantity of Carbon nano particles in polymers, improve different properties of a polymer - converting otherwise non-absorptive material to a good microwave radiation absorber. The materials may include Carbon nanotubes (CNTs), Carbon fibers (CF), Graphene etc. [18-20]

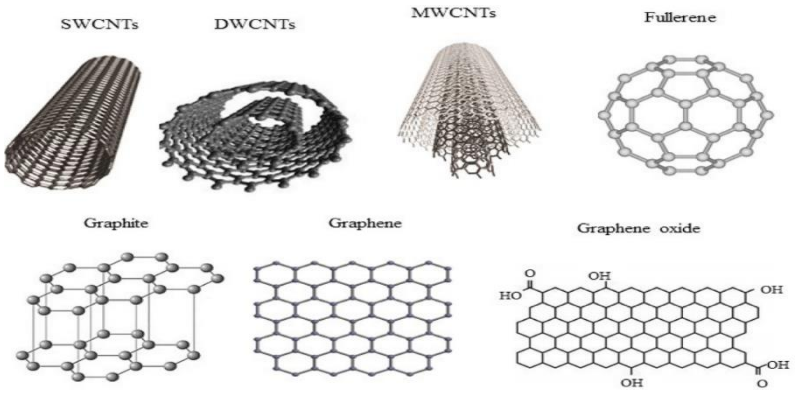


Fig 1.3. Different structures of carbon nanomaterials [21]

**Carbide based nanocomposites:**

Silicon Carbide (SiC) is foundation for the nanoparticles in this class. Other materials like Al/SiC, Ni/SiC etc., derived by SiC has shown good absorbing properties. [22]

**Oxides based nanocomposites:**

These are important nanomaterial with respect to their response in GHz frequency range. Few examples are Iron Oxide, Titanium Oxide, Manganese dioxide, Silicon Oxide, Graphene Oxide, Boron Oxide etc [23-25]

**Sulphide based nanocomposites:**

Metal sulfides are significant microwave absorptive materials because they are thought to produce relatively high reflection losses. Important examples are the sulphides of molybdenum, tungsten, copper, and manganese. [26-27]

### 1.11 Applications for Microwave absorbing Materials

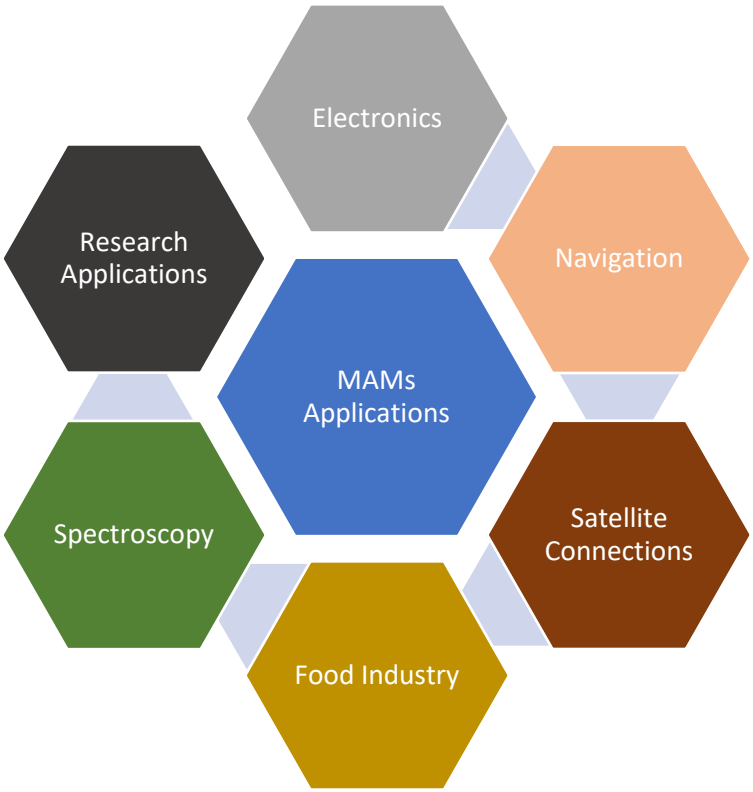


Fig 1.4: Applications of microwave absorbing materials [28]

# Chapter 2: Literature Review

**Progress of Nanomaterials in Microwave Absorption:**

The speedy progress and extensive proliferation of microwave the radio frequency communication systems have resulted in a significant surge of electromagnetic spectrum within the living surroundings. (Muhammed and Muhammad Z. Iqbal, 2021). The increase in microwave sources can be attributed to advancements in communication methods, including mobile phones, laptops, and antennas used in aviation and automobiles. Recently, research efforts have been dedicated to finding solutions that ensure shield from electromagnetic (EM) radiation. EM absorbing materials have been developed to address these concerns and safeguard public safety, including support secure military procedures. Extensive research has been conducted on various types of EM absorbing materials, particularly composite materials. These materials involve incorporating absorbing charges (magnetic or dielectric) into a present matrix material. Carbon allotropes for instance graphene, M-Xenes, carbon nanotubes and carbon fibers have garnered significant devotion due to their lightweight nature and their effectiveness in electromagnetic interference (EMI) shielding. This study gives a complete overview of present research progress for utilization of nanomaterials. [29]

**2.1 Influence of sample thickness and concentration on absorption:**

A composite material was developed by Hussein, Jehangir, and their team in 2020, which included functionalized multi-walled carbon nanotubes, polyurethane, and different concentrations of these materials like Cobalt Oxide. The researchers conducted experiments on nine samples to determine their microwave absorption capacity, covering a frequency range of 5-50GHz. Their findings revealed that the composite that contained 20% CoFe functionalized CNT/PU exhibited the highest reflection loss of -45dB between the frequencies of 15-20 GHz. [30]

In 2020, Singh, Kumar, and Singh noted an improvement in the microwave absorption of SiC nanocomposites by adding a small quantity of SWCNTs in the Ku band of the electromagnetic spectrum. Their study found that a thickness of 2.5mm resulted in a reflection loss of -37.11 dB at a rate of recurrence of 14.23GHz. [31]

In 2019, Zhu evaluated several effective medium theories to create a polymer-based nanocomposite consisting of Ba1−xSrxTiO3 (BST) and $Ni_{0.5}Zn_{0.5}Fe_2O_4$/Ni-Fe (NZF) in CST Microwave Studio. He

then computed the permittivity and permeability of the composite material from the 1-4 GHz region. Zhu stressed that utilizing CST MWS could lead to improved outcomes when measuring the dielectric characteristics of dielectric materials.

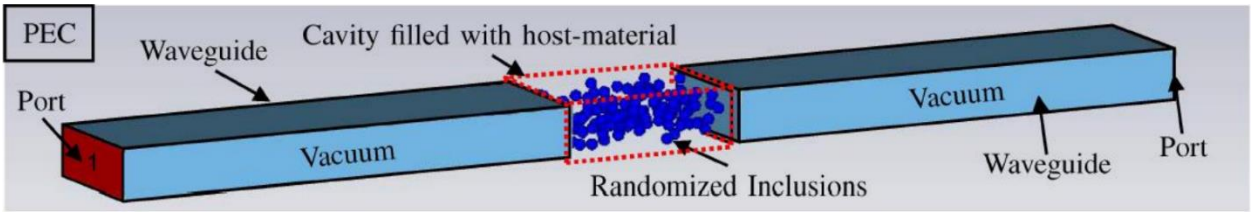


Fig 2.1. Diagram of waveguide for Simulation [47]

Guo, Jiang, Fu, and Research (2018) synthesized modified [(1-x)$MnO_2$-xMWCNTs] /waterborne Polyurethane composites that presented not only good microwave absorption properties but also better thermal stability and mechanical strength. Out of different samples the one that contained 20% MWCNTs showed the maximum reflection loss of -28.7dB at 6.4 GHz frequency range. The model thickness was 2.5mm. The microwave absorption value decreased with increase in concentration of MWCNTs in the composite. [32]

**2.2 Dielectric Properties of MAMs:**

In 2006, Koledintseva and colleagues investigated the frequency-dependent properties of composites that incorporated 3D randomly oriented conducting shapes or nanorods at optical frequencies. To model these composites, they utilized the Maxwell Garnett formulation. The primary influence on the frequency-reliant permittivity of the blend was the conductivity of the metal enclosures. However, it was observed that the performance of metal enclosures at ophthalmic frequencies differed significantly from their behavior at microwave frequencies. Additionally, the mean free path of electrons in metals could be smaller than the characteristic size of the metal inclusions, resulting in a considerable reduction in the conduction of the metals. By incorporating all these influences, the Maxwell Garnett mixing formulation offered a wide range of possibilities for creating composite materials with frequency-dependent properties that contain conducting particles. [33]

In 2019, Yakovenko and colleagues conducted experimental tests on composites composed of MWCNTs/Epoxy in a frequency range of 1-67GHz to determine their dielectric properties. They also computed the effective permittivity of different volume fractions of composites, considering the aspect ratio of nanotubes, using the Maxwell Garnett mixing model for nanocomposites. The results

obtained from the experimental and calculated tests only matched at a volume fraction as small as 0.006%. This study emphasized the significance of the interface linking the matrix and nanofiller particles in influencing the dielectric stuffs of nanomaterials. [34]

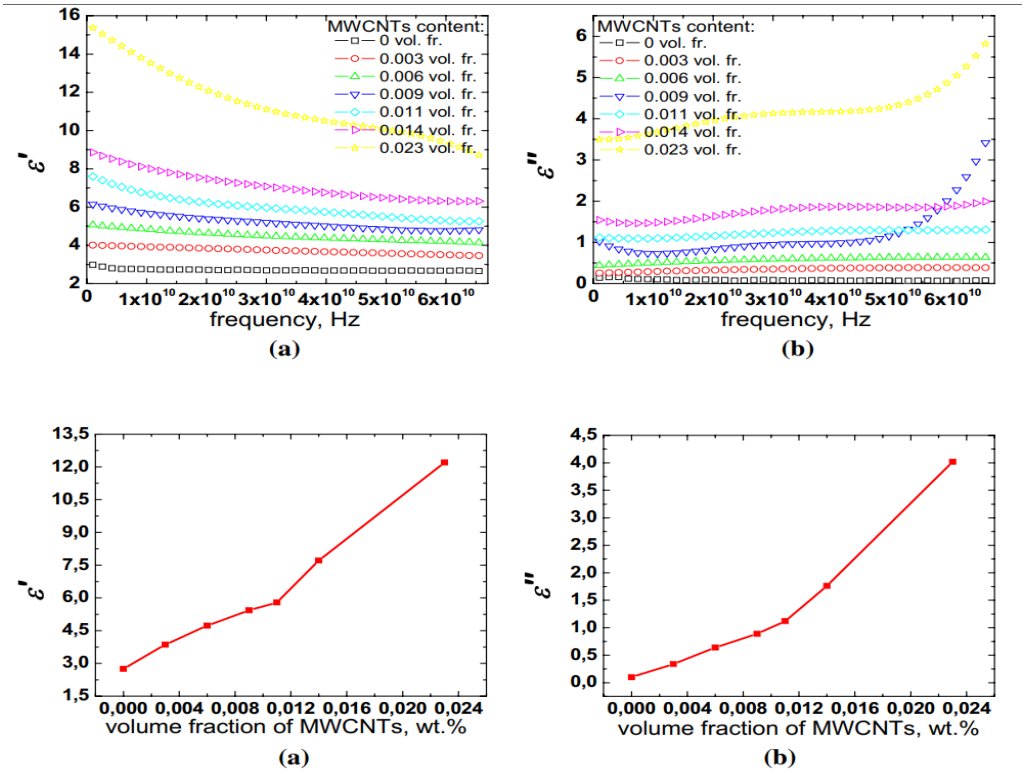


Fig 2.2. Conc for dependencies of the dielectric permittivity for MWCNTs/CMs (a) and imaginary (b) parts of permittivity

### 2.3 Effects on Morphology and Structure

In 2019, Savi, Giorcelli, and Quaranta used simulations to analyze microwave absorbing nanocomposites created from MWCNTs (4 wt%)/epoxy resin techniques that were equipped and illustrated. Previous research had investigated the correlation between MWCNT dilution, dispersion, and permittivity. The researchers fabricated 2mm thick single layer absorbing material and subjected it to microwave reflection tests. The interfacial polarity of MWCNTs with high aspect ratios and specific surface areas developed in a decrease in mixture reflection coefficient at 6GHz. The microwave absorption in MWCNT epoxy resin composites was determined by the aspect percentage which e, definite surface band, and transparency of the MWCNTs. [35]

Fe3O4 nanoparticles spread on single-walled carbon nanotube (SWCNT) blend were studied by Rambabu Kuchi and Hieu M. They discovered that the Fe3O4/SWCNT composite exhibited a well-defined structure and a compelling microwave absorption of -36.96 dB at 10.49 GHz. The efficient absorption was showed to the successful integration of magnetic nanoparticles ($Fe_3O_4$) onto the SWCNT. This research suggests a cost-effective approach to producing Fe3O4/SWCNT composites that exhibit excellent microwave absorption properties. [36]

In their research, Pritom J Bora1 and K J Vinoy used to follow on studying the properties of polymer nanocomposite films for electromagnetic interference (EMI) blocking. Specifically, they processed a composite solution of polyaniline (PANI) and manganese dioxide (MnO2) nanorods and evaluated the EMI shielding effectiveness (SE) is the resultant film in both the X-band range (8_12 GHz) and Ku-band range (12_18 GHz) frequency ranges. The researchers found that the PANI/MnO2 nanorods composite film exhibited an impressive SE of -35dB in the X-band, that is mainly caused by EMI shielding through absorption (SEA) of -24 dB and EMI shielding through reflection (SER) of -11 dB. In the Ku-band, the film displayed an even more effective SE of -39 dB.

Moreover, the study investigated several other properties of the film related to EMI shielding, including conductivity, depth of penetration, and electromagnetic (EM) attenuation constant. The dielectric assets of the film were also examined. Overall, the results suggest that the PANI/MnO2 nanorods composite film has great potential as a economical solution for EMI shielding in the range of Ku_band and X_band frequency. [37]

$MnO_2$ empty microspheres comprised of nanoribbons were effectively assembled via a superficial hydrothermal method with $SiO_2$ sphere templates. Powder X-ray diffraction (XRD), transmission electron microscopy (TEM), and a vector network analyzer were used to study the samples as they were made. The dialectical possessions for the 3D manganese dioxide empty microspheres are efficient than the 1D nanoribbons. Compared to 1D MnO2 nanoribbons, MnO2 microspheres are also much better at absorbing microwaves in the X (8.12 GHz) and Ku (12.18 GHz) bands. With a thickness of only 4 mm, a hollow microsphere has a minimum reflection loss of -40 dB at 14.2 GHz and a minimum reflection loss of -10 dB at 3.5 GHz. The possible mechanism for the improved ability to absorb microwaves is also talked about. [38]

Bien Dong Che *et al*. (2015) apply nanocomposite that was made by mixing three different kinds of MWCNTs (Baytubes C150P, Nanocyl NC7000, and VAST) with epoxy resin. To make the

dispersions, they used two simple methods: the solution dispersion method and the ball milling method. They pointed out that Nanocyl NC7000 worked better as a microwave absorber in the X-band range of frequency no matter what method was used. For bulk composite formation, however, they found that the ball milling method was better than solution dispersion because it didn't require the mechanical agitation and solvent evaporation that solution dispersion did. [39]

Wen Hong *et al.* (2015) studied by pouring, carbon fiber-strengthened epoxy resin composites are made. The nonconductor assets of carbon fiber-reinforced epoxy resin mixture with changed fibre content and length have been tested at frequencies from 8.2GHz to 12.4GHz. The real and imaginary permittivity of composite goes up as fibre length goes up, which is because the depolarization field goes down, and it goes up as the volume fraction goes up, which is because the polarisation goes up. A formula for the Reynolds-Hugh theory to figure out the effective permittivity of CFs composites. Experiments have shown that the formula works. The proposed formula is then used to figure out the axial permittivity of CFs and figure out how the length of the fibre affects the axial permittivity. [40]

Hualiang Lv, Ji, Liang, Zhang, and Du (2015) they have made a new three-part material out of MnO2/Fe/graphene. First, a simple liquid process was used to make a strip of MnO2 that was 30 nm wide and shaped like a rod. The ternary composite that was made had the best reflection loss of equal to -17.49 dB, which was achieved with in frail coating texture of 1.5mm. This was capable to meet the constraints of being light and absorbing a lot of light. The effective frequency range of MnO2/Fe–GNS is wider than that of basic $MnO_2$ or $MnO_2$/Fe. This may be because it has a moderate ability to match impedance and reduce power. [41]

Wang and Zhao (2013), along with other researchers, looked at MWCNTs-epoxy composites. We looked at the microstructures, dielectric constants, and how well the MWCNTs-epoxy composite samples absorbed microwaves. The results for the simulation showed that the amount of MWCNTs in the composites has a big effect on how well they absorb microwaves. For samples with 8–10 wt% MWCNT loadings, the microwave absorption fraction spread up to 20_26 percent around 18_20 GHz. The high absorption performance is mostly due to the fact that MWCNTs can absorb microwaves and that MWCNTs-epoxy composites have a high dielectric loss. [42]

Liang, Yang, and Choi (2012) look into how irregularly shaped manganese dioxide particles (NP) and manganese dioxide nanorods (NR) absorb electromagnetic and microwave waves at 2_18 GHz. In complex permittivity real part ranged from 7.8 to 9.6 for a 60 wt% MnO2 NP-epoxy composite,

but it was 6.6 to 10.0 for a 12 wt% MnO2 NRepoxy absorber. The MnO2 NR-epoxy absorber has a dielectric loss tangent that is bigger than the of the MnO2 NP-epoxy combination. The 3mm thickness sample gives lowest reflection loss is -11.59 dB at 9.11 GHz for a 60 wt% manganese dioxide epoxy absorber and 20.7% at 9.6 GHz for a 12 weight percentage $MnO_2$ NR-epoxy absorber. [43]

The carbonyl iron/MnO2 composite was looked at by Wuqiang Zhang et al (2014). A scanning electron microscope (SEM) was used to describe the shapes a scanning electron microscope (SEM) was used, and a vector network analyzer was used to measure how microwaves were absorbed in the range of 2–18 GHz. When the amount of MnO2 in the composites went up to 30% by weight, the minimum reflection loss reached 39.1 dB at 4.4 GHz and a thickness of 3.5 mm. The good electromagnetic match and the fact that both dielectric loss and magnetic loss were present could explain why the composites were better at absorbing microwaves. The results of the tests showed that carbonyl iron/MnO2 composite is a good candidate for a material that can absorb microwaves, specifically in the S_band (2–4 GHz) and C_band (4–8 GHz). [44]

Decrossas, Sabbagh, Hanna, and El-Ghazaly (2011) looked at carbon nanotubes (CNTs) with different densities over a wide range of frequencies, from 10 MHz to 50 GHz. The extraction method is based on a strict modelling of coaxial and circular discontinuities using a mode matching technique and an inverse optimization method to map the simulated scattering parameters to those measured by a vector network analyzer. The percolation theory explains how the large parameters of complex permittivity found at minimal frequencies are probable. To confirm what was found before, the effective permittivity of a mixture of nanoparticles of alumina and CNTs is studied as a role of frequency and packaging intensity. [45]

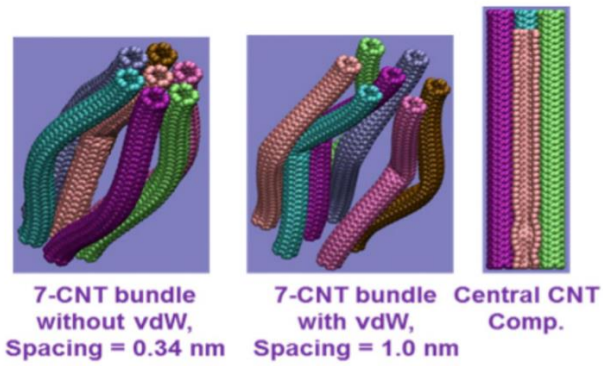


Fig 2.3. Molecular Dynamics Models of Single-Walled Carbon Nanotube Packs Under Automated Loading [46]

Sucheng Li *et al*. (2012) investigate on Maxwell Garnett's effective medium technique that was used to figure out how complex a material's effective permittivity is. In their experiments, researchers made composites with different amounts of solid particles mixed into silicone oil. Using the MG mixing formula, they were able to figure out the permittivity of the solid inclusions from the measured permittivity of the oil and the composite. The process doesn't have to take into account the shape of solids, and measured values for alumina, glucose, and pearl have also been confirmed by experiment. [47]

Sun, Gao, Li, Wu, and Yellampalli (2011) *et al*. looked at how well MWCNTs doped with rare earths and aligned nanotubes absorbed microwaves in the 2–18 GHz range. They found that adding 1% rare earths to carbon nanotubes made them better at absorbing microwaves in the X-band range. At 10.88 GHz, these had a reflection loss of -29 dB. On the other hand, the aligned nanotubes were better at absorbing sound at higher frequencies (2-18GHz). [48]

Folgueras, Alves, Rezende, and Management (2010) studied that paints and sheets that absorb electromagnetic radiation are made of magnetic and dielectric materials that are mixed with polymers. Using polyurethane as a base, two different kinds of paint were made with carbonyl iron and/or polyaniline. Polyaniline conducting polymer was also used as a filler to make silicone sheets. The materials were also tested for their ability to let electricity through and let magnets pass through. Simulations were run on the silicone sheets to find a link between the effective permittivity and the thickness of the material. The paints took in 60–80% of the electromagnetic radiation that hit them, while the silicone sheets took in 90%. This displays that the material has the potential to understand radar. [49]

Koledintseva, Drewniak, DuBroff, Rozanov, and Archambeault (2009) analyse composites that are used in many engineering uses, exceptionally for the design of microwave shielding insertions to make sure they are electromagnetically compatible. Researchers look at shielding structures with both layers that absorb and layers that reflect. Composites with fibres are being thought about. Maxwell-Garnett theory is used to model composites that absorb light but have a low number of conducting cylinder inclusions, Maxwell-Garnett theory is used. The McLachlan formulation is used when the number of inclusions in a layer is close to or above the percolation threshold. This is the case for reflecting layers. The Debye curves use a curve-fitting method, specifically a genetic procedure, to get an idea of how frequency affects an effective permittivity. [50]

Z. Kucerova *et al*. (2009) examine that a matrix of polyurethane (PU) were made with different carbon nanofillers and changing amounts of fillers so that their structure, mechanical properties, and ability to absorb microwaves could be studied. Carbon microfibers, flat carbon microparticles, and multiwalled carbon nanotubes (MWNT) were all used as fillers. Scanning electron microscopy and transmission electron microscopy were used to look at the structure of the composite on a small scale. The depth sensing indentation test was used to find out the material's systematic assets, for instance its overall density, elastic modulus, and the creep. Researchers looked at the different properties of PU composites with varying nanofillers. Composites always had high density, creep resistance and elastic modulus than PU that wasn't filled. The shape, content, and distribution of the filler were also investigated. [51]

| | | | |
|---|---|---|---|
| Pure PU | 3.1 | 0.03 | 0°33′ |
| Filler | $\varepsilon_r$ | $\varepsilon$ | $\delta$ |
| Filled polyurethane | | | |
| Carbon microparticles 0.5 wt.% | 3.33 | 0.09 | 1°29′ |
| Carbon microfibers 0.5 wt.% | 5.00 | 0.92 | 10°24′ |
| MWNT 0.05 wt.% | 3.72 | 0.28 | 4°16′ |
| Carbon microparticles 1 wt.% | 8.63 | 2.73 | 17°33′ |
| Carbon microfibers 1 wt.% | 15.23 | 6.04 | 21°37′ |
| MWNT 0.1 wt.% | 4.38 | 0.61 | 7°57′ |

Fig 2.4. Complex permittivity values, d corresponds to loss angle [52]

## 2.4 Effect of Heat on MAMs

Researchers have been looking into how temperature affects the stability of composites used as MAMs for the past ten years.

Liew, K *et al*. (2005) concluded that, molecular dynamics modeling and in Berendsen thermostat proposal, the stability of atomic structure and variation of single-walled CNTs and multi-walled CNTs was used to analyze. Closed single walled carbon nanotubes are modeled first and modelled all collectively with open resulted single walled CNTs. They discovered that the temperature at which they can quantized is less than 5% change. Additional CNTs are then modeled as open-ended. The outcome show that CNTs with larger lengths dt and smaller lengths L can survive thermal loads better than those with smaller diameters dt. Longer CNTs tend to bend, causing the end-to-end distance to shrink. The multi-walled CNTs are, however, not as thermally constant as single-walled CNTs appropriate to the existence of more than single layer in multi-walled CNTs. When a multi-walled CNT is exposed to thermal load, the atoms from changed layers start to vibrate. At high temperatures, the pulsations become larger and the atoms from one layer strike with the atoms from the neighboring layers. The multi-walled CNTs to break, this makes it easier. [53]

Tinsley, D. M., & Sharp, J. H. (1971) examine that in nitrogen, air, and oxygen, TG and DTA arcs of $MnO_2$ have been made. The reaction was seen in the ranges of 450 to 600 and 750 to 1100, and the partial pressure of oxygen changes the decomposition temperatures. At 1200, the endotherm is not affected by the air and does not lead to weight loss. So, it's not because MnO formed, but because $Mn_3O_4$ changed into different forms. TG showed that MnO formed when nitrogen was heated above 1400, but this did not happen when oxygen was heated to 1500. [54]

## 2.5 Gap Identification

Many studies have been conducted on materials that can absorb microwaves. New shielding materials have been created and characterized with the use of nanotechnology. However, researchers are still trying to develop novel and efficient materials and nanocomposites for microwave absorption tendency required by electronics and defense industry.

It is observed that ferrite elements have the highest absorption efficiency, but it tends to be oxidized due to temperature. In this case weight of the material also increased. For this carbon nanotubes, polyaniline, etc. are preferred in microwave absorbing materials.

Computer simulations are not performed on the prediction of microwave absorbing materials for different thickness.

### 2.6 Problem Statement

Metal-based nanomaterials have been employed as Microwave Absorbing Materials (MAMs). Unfortunately, these materials are heavy, prone to clumping together, sensitive to high temperatures and have a strong affinity to oxide. Consequently, their usage as MAMs is severely restricted. Therefore, there is a significant demand for MAMs that are light weight, have a small thickness, exhibit strong chemical stability, offer a broad absorption frequency range and deliver excellent absorption performance.

### 2.7 Significance of current research

MAMs have been widely researched to regulate electromagnetic radiation from electronic devices due to new regulations on compatibility and interference. MAMs are also significant tools in electronic combat because they can be used to hide possible objects from radar. Also, microwave absorbing material are often used to hide the walls of chambers anechoic and stop or decrease the electromagnetic polarization from with huge structures like aero planes, ships, and tanks.

The research aims at how the two composites behave in the frequency ranges already mentioned. The thickness of the sample taken is used to compare the two things. Through effective medium theories, the method used in this study can be used to find out the effective assets for nanocomposites, for example their permeability and permittivity. Model developed in this project has the potential to be utilized in any research study where different frequency ranges provide effective permittivity and permeability quantities of a material. The model can help determine the effectiveness of a shield by computing the scattering parameters.

### 2.8 Objectives

- To design materials that absorb microwaves very well (8GHz-18GHz) and can be used in guidance systems.
- To figure out the reflection loss (in dB) for MAMs that are used as good absorbers (8GHz-18GHz) based on their permittivity and permeability values.
- To find out the effect of material thickness at scattering parameters, reflection loss values.

# Chapter 3: Material and Methods

In this study, we wanted to see how I Molybdenum diselenide (MoSe2) with Alumina and (ii) Molybdenum diselenide (MoSe2) with Molybdenum disulfide (MoS2) reacted to microwaves. The scattering parameters S11 and S21 were found using Computer Simulation Technology for Microwave studio CST_MWS 2019. CST studio is derived on Maxwell's electromagnetic equations.

## 3.1 Electromagnetic Theory

In 1865, James Clerk Maxwell suggested that electric currents and charges make electric and magnetic fields, and that the electric ground makes the magnetic ground, and the magnetic ground makes the electric field. In his theory, he was able to bring together the ideas of electricity, magnetism, and light. Electromagnetic theory is a set of four equations that explain how electromagnetic forces interact. The math equations that are proposed by J.C. Maxwell, are based on the math and experiments done by Ampere, Michael Faraday, and Gauss before them. Oliver Heaviside's work is what gave these equations their current form. He simplified them and limited them to electric and magnetic domains and their sources. Both the distinction and integral types of these equalities are used. The equations show how electric and magnetic fields are made by the way charges are spread out and how their strengths change over time. [55-57]

The differential form of equations is:

$$\nabla \times \bar{H} = \frac{\partial \bar{D}}{\partial t} + \bar{J} \quad (1)$$

$$\nabla \times \bar{E} = -\frac{\partial \bar{B}}{\partial t} \quad (2)$$

$$\nabla . \bar{D} = \rho \quad (3)$$

$$\nabla . \bar{B} = 0 \quad (4)$$

In these equations:

$\bar{E}$ is the Electric field vector (volts / meter), $\bar{H}$ the magnetic field vector (Ampere / meter), $\bar{D}$ the electric flux density vector (Coulombs / meter$^2$), $\bar{B}$ magnetic flux vector (Webers / meter$^2$), $\bar{J}$ current density vector (Ampere / meter$^2$) and ρ is the Volume charge density (Coulombs / meter$^3$)

Using the additional integral form of the Maxwell equations makes it easy to understand what they mean in terms of physics. Using Stoke's Theorem, equations 1 and 2 can be changed to integral form. Equations 3 and 4 can be changed to integral form by using Divergence Theorem.

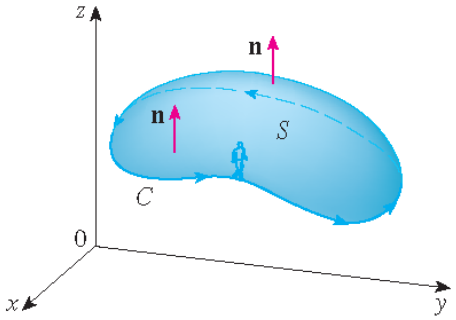


Fig 3.1. Stoke's Law

When we take integration of these equations, they become.

$$\int_l \bar{H} \cdot d\bar{l} = \oint_a \left(\frac{\partial \bar{D}}{\partial t} + \bar{J}\right) \cdot d\bar{a} \qquad (5)$$

$$\int_l \bar{E} \cdot d\bar{l} = \oint_a \frac{\partial \bar{B}}{\partial t} \cdot d\bar{a} \qquad (6)$$

$$\int_S \bar{D} \cdot d\bar{a} = \int_V \rho \; dV \qquad (7)$$

$$\int_S \bar{B} \cdot d\bar{a} = 0 \qquad (8)$$

### 3.2 Dielectric Properties

Dielectrics are materials that don't conduct electricity but tend to store electric charges and become polarized when exposed to an electric field from the outside.

#### i. Polarizability

The charges on the perfect dielectrics can't be taken away by the electrical field outside of them. Charges that are in an electric field move just a little bit from their average position. This is how they try to make polarization. At the same time, however, an opposing force called a "restoring force" tries to stop this movement of charges from where they should be. The amount of movement between positive charges, which move toward the electric field, and negative charges, which move away from it, depends on which of the two forces is stronger. The distance between these two charges is equal to the moment of dipole that is made. Because an electric field causes polarization, dielectrics can store electrical energy in them.

In the same way, magnetic materials show magnetic polarization when exposed to an electrical or magnetic field from the outside.

There are different types of polarizations because different materials can have different ways of distributing charges. Like atomic, ionic, orientation, and interfacial polarization. Each type corresponds to a different range of frequencies and can also be material specific. For example, only ionic compounds can show ionic polarization. In the same way, orientation polarization happens at low frequencies, while electronic polarization happens at higher frequencies, such as for infrared frequency range. Most materials for the microwave frequency range go through a process called dipolar or orientation polarization. [58]

**ii. Complex Permittivity & Permeability**

Complex permittivity or dielectric constant tells that how much of energy from the wave is stored in a composite material, whereas Maxwell equation no. 1 & 2 are:

$$\nabla \times \bar{H} = \frac{\partial \bar{D}}{\partial t} + \bar{J} \quad \text{(9)}$$

$$\nabla \times \bar{E} = -\frac{\partial \bar{B}}{\partial t} \quad \text{(10)}$$

In a vacuum, the equations for electric ground E and magnetic ground B are

$$D = \varepsilon_0 E \quad \text{(11)}$$

$$B = \mu_0 H \quad \text{(12)}$$

Wherever $\varepsilon_0$ is the permittivity of planetary having value $8.85 \times 10^{-12}$F/m and $\mu_0$ is the permeability of free space having value $1.2566 \times 10^{-6}$ H/m. In a material, these relationships are not quite as simple as they seem and become:

$$D = \varepsilon_0 E + P \quad \text{(13)}$$

(P is the polarization factor)

$$B = \mu_0 H + M \quad \text{(14)}$$

(M is the magnetic polarization factor)

Polarization P is directly connected to the electric ground E, and magnetic polarization is directly correlated to the magnetic field H:

$$P = \chi_e \varepsilon_0 E \quad \text{(15)}$$

($\chi_e$ is the electric susceptibility)

$$M = \chi_m \mu_0 H \quad \text{(16)}$$

($\chi_m$ is the magnetic susceptibility)

With the help of Ohm's Law ($J = \sigma E$) and the Maxwell equations in a time-harmonic field, we can find the complex permittivity value as

$$\varepsilon = \acute{\varepsilon} - j\check{\varepsilon} \quad \text{——————————} (3.1)$$

$$\varepsilon = \varepsilon_0 (\acute{\varepsilon}_r - j\check{\varepsilon}_r) \quad \text{——————————} (17)$$

Where σ is conductivity for the material, έ is the real part of permittivity and ε̌ is imaginary part. Real part concerns the medium's capacity to store energy, whereas the imaginary part concerns its potential to lose energy.

Following a same procedure on eq. 2, we obtain:

$$\mu = \mu' - j\,\mu'' \quad \text{——————} \quad (3.2)$$

$$\mu = \mu_0(\mu'_r - j\mu''_r) \quad \text{——————} \quad (18)$$

Dissipation factor, commonly referred to as a dielectric constant (tanδ), is another key parameter. As it is the ratio between imaginary and real part, i.e.

$$\tan\delta_e = \varepsilon''/\varepsilon' \quad \text{——————} \quad (19)$$

For magnetic loss tangent the equation is:

$$\tan\delta_m = \mu''/\mu' \quad \text{——————} \quad (20)$$

Permittivity and permeability are two qualities that change depending on the frequency of an electromagnetic field. [59-60]

**iii. Dispersion and Relaxation in Dielectrics**

Dispersion refers to the frequency dependency of complex permittivity and permeability. To investigate how real and imaginary permittivity values change with frequency, the Kramers-Kronig relation is applied.

Relaxation is the process by which a dielectric adjusts its polarization when subjected to an electric field. For instance, the dipoles in a material have enough time to rotate and keep in touch the change in electric field at low frequencies like the microwave frequency, but at higher frequencies the actual permittivity (έ) of the material decreases as individual dipoles can't keep in step with changing external field. [61]

**3.3 Shielding Effectiveness**

The competence of a material to block electromagnetic radiations are called its shielding effectiveness (SE). It is measured by how much the intensity of electromagnetic radiations drops as they pass through the shield. Due to a contrast in resistance between the wave that hits the shield and the shield, some of the wave is reflected at the interphase. The name for this is Reflection Loss (RL). The amount that the shielding material takes in is called the "Absorption Loss." The main thing that happens in absorption loss is that heat is made by the material because it has dipoles (electric, magnetic or both depending on type of material). Multiple reflections within the material weaken a part of the wave that hits it. Mathematically, we can figure out how well a shield works as [62-64]

$$SE_{Total} = SE_{Reflection} + SE_{Absorption} + SE_{Multiple\ reflection} \quad (21)$$

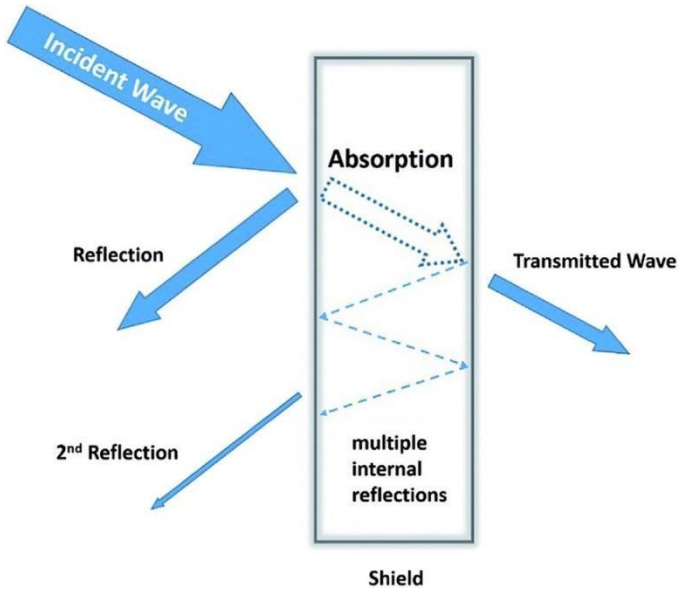


Fig 3.2. Schematic of EMI Shielding Mechanism [65]

Most of the time, the multiple internal reflection factor is ruled out at frequencies of 1GHz or higher. So, you can write total shielding as:

$$SE_T = SE_R + SE_A \quad (22)$$

$SE_R$ & $SE_A$, the values are calculated in relationship of Reflectivity and Transmission

$$SE_R = 10\log (1/1-R) \quad (23)$$

$$SE_A = 10\log (1-R/T) \quad (24)$$

Putting equation no. 23 & 24 in equation no. 22, will give total shielding as

$$SE_T = 10 \log (1/T) \quad (25)$$

The quantities of Reflectance (R) and Transmittance are calculated through Scattering Parameters as:

$$R = |S11|^2 = |S22|^2 \quad (26)$$

And

$$T = |S12|^2 = |S21|^2 \quad (27)$$

### 3.4 Effective Medium Theories

It is already common knowledge that shielding materials can be made from composites consisting of a dielectric matrix with conductive inclusions. Various effective medium theories are applied to the evaluation of the composite's effective qualities.

**Maxwell Garnett Effective Medium Theory**

Maxwell-effective Garnett's medium theory for homogeneous mixtures is the most well-known and widely applied of these approaches. The effective permittivity of a mixture containing rod-shaped inclusions varies as a role of frequency. Electromagnetic parameters for matrix and the enclosures are required for using the effective medium theory. [66]

Maxwell Garnett multiphase formula to find effective permittivity of composite with various concentrations of inclusions is:

$$\varepsilon_{eff} = \varepsilon_m + \frac{\frac{1}{3}\sum_{i=1}^{n} v_f \left(\varepsilon_f - \varepsilon_m\right) \sum_{k=1}^{3} \frac{\varepsilon_m}{\varepsilon_b + N_{ik}(\varepsilon_f - \varepsilon_m)}}{1 - \frac{1}{3}\sum_{i=1}^{n} v_f \left(\varepsilon_f - \varepsilon_m\right) \sum_{k=1}^{3} \frac{N_{ik}}{\varepsilon_b + N_{ik}(\varepsilon_f - \varepsilon_m)}}$$

Here

$\varepsilon_m$ = Relative Permittivity of a Matrix Dielectric

$\varepsilon_f$ = Relative Permittivity of nanofiller

$v_f$ = Volume fraction of the filler

$\mathbf{N}_{ik}$= Depolarization factor

***K*** = corresponds to Cartesian coordinates

To evaluate depolarization factor following formulae used are: [67-68]

$$N_x = \frac{(1-e2)}{2e3}\left(ln\frac{(1+e)}{(1-e)} - 2e\right)$$

$$N_y = N_z = \frac{1-Nx}{2}$$

$$e = \sqrt{1-\left(\frac{2r}{l}\right)^2}$$

### 3.5 Microwave Absorbing Materials and their Properties.

Under the conditions of this work, nanocomposites have been created using the following matrix and nanofiller.

| **Matrix** | **Nano Fillers** |
|---|---|
| Molybdenum diselenide ($MoSe_2$) | Alumina ($Al_2O_3$) |
| Molybdenum diselenide ($MoSe_2$) | Molybdenum disulfide ($MoS_2$) |

**Properties of Polymer Matrix:**

| **Polymer** | **Young's moduli** | **Shear Strength** |
|---|---|---|
| $MoSe_2$ | 100.9 GPa | up to 60 GPa |

**Properties of Nano fillers:**

| **Nano fillers** | **Length (mm)** | **Width (mm)** | **Hight (mm)** |
|---|---|---|---|
| Alumina | 22.86 | 10.16 | 1 |
| $MoS_2$ | 22.86 | 10.16 | 1 |

### 3.6 Methodology

We used the MGarnett equations to use relative permittivity to find the effective permittivity of the material containing a nanofiller at a volume proportion of 0.4%. Two nanofiller composites and two fullerene composites were designed i.e., $MoSe_2$ combining with the matrix (Alumina and $MoS_2$).

#### i. CST Microwave Studio

If we need to develop, analyze, or optimize a system's performance in the electromagnetic frequency spectrum, CST Microwave Studio is the tool for us. The high frequency simulation operations in CST microwave studio are completed using a variety of techniques. Frequency Difference Time Domain (FDTD), Finite Element Method (FEM) both are the part of Finite Integration Technique (FIT). The solutions for the electromagnetic Maxwell equations used in the program can employ either of the two previously discussed approaches.

To learn about the nanocomposites, microwave absorption properties in the X-band region (8- 12 GHz) and the Ku - band region (12-18 GHz) for microwave spectrum, we developed them in CST_MWS suite 2019.

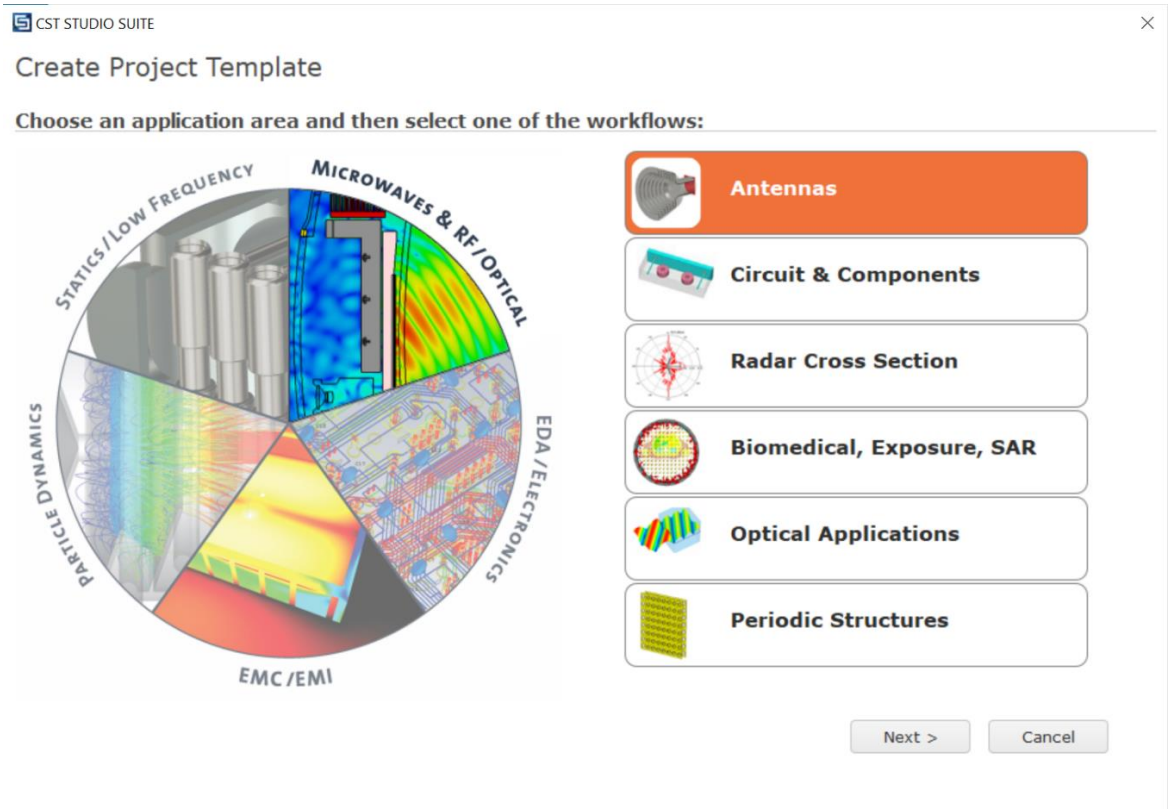


Fig 3.3. CST Microwave Studio Suite 2019

### ii. Wave Guide Models

Many techniques are used to determine the permittivity of microwave-absorbing materials. Using rectangular waveguides is one such method. Scattering parameters are determined by transmitting electromagnetic radiation through the waveguide at the desired frequency range, after which the SUT is carefully positioned within the waveguide. The literature provides the dimensions of these waveguides. [69]

Microwave absorption simulations use 3D models of such waveguides to get scattering parameters. We did this by simulating the behavior of two distinct waveguides operating throughout the scales of 8–12 GHz and 12–18 GHz, respectively.

### iii. Setting Up the Simulations

### 8.2 – 12.4 GHz Range

Sizes of 22.86mm and 10.16mm were chosen for the inner opening of the waveguide to operate in this frequency range. Perfect Electric Conductor (PEC) was used as the source material. For calculating scattering parameters with a hexahedral mesh, the time domain solver was chosen.

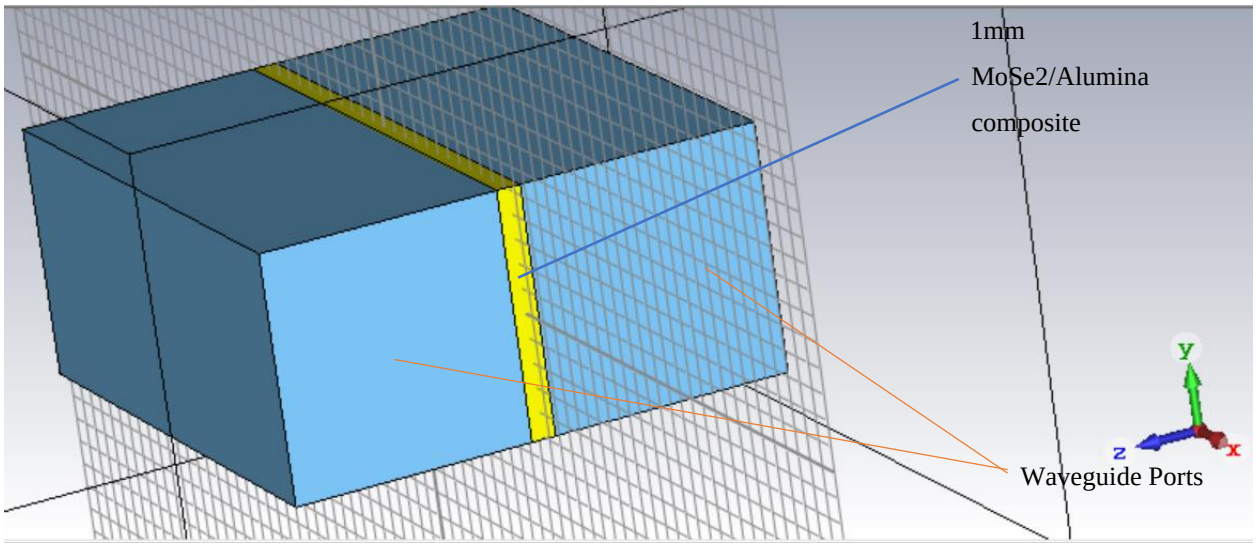


Fig 3.4. Waveguide model containing 1mm $MoSe_2$ with Alumina Composite - a CST Model

### 12.4 – 18 GHz Range

The inside dimensions of the two waveguides were 15.79mm in length and 7.89mm in breadth. The foundation was assumed to be an ideal electrical conductor. In the middle of the two waveguides, samples of composite $MoSe_2$ bundles with alumina and $MoSe_2$ bundles with $MoS_2$ were taken. The two ports in the waveguides were cut out of the waveguide's opposing sides. Scattering parameters were calculated after running the simulations with electric boundaries.

# Chapter 4: Results and Discussion

The end results presented in this section are divided into different parts.

a. The study of Reflection Loss and Shielding effectiveness in 8–12 GHz range (X-Band Studies)
b. Reflection Loss and Shielding effectiveness studies in 12–18 GHz range (Ku–Band Studies)
c. Analyzing results for $MoSe_2$ and Alumina Composites side by side.
d. Conclusion

### 4.1 EMI Shielding in X – Band Studies:

Two composites are addressed to their effective permittivity (ε), reflection loss (RL), and shielding effectiveness (SE).

1. $MoSe_2$/ Alumina
2. $MoSe_2$ / $MoS_2$

**Effective Permittivity**

How much microwaves can penetrate a material is determined by the real component of permittivity (ε′), whereas the storage tendency of the penetrated radiation is determined by this imaginary portion (ε″). While the ability of a material to dissipate energy into heat is measured by a quantity called the dissipation factors. An optimal shielding material will have a well-rounded set of characteristics across all three categories ε′, ε″ and tanδ. [70]

When a filler is contained into a polymer medium, the permittivity for both the matrix and the filler undergoes variations. This means that the resulting composite has a different permittivity value than either of the original materials. Therefore, the changed values enhance the composite material's EMI shielding capability. [71]

These permittivity values for MoSe2/Alumina and MoSe2/MoS2 composites are depicted in the following figures. The following graph contain the results of applying the Maxwell-Garnett mixing formula to generate these values given below.

$$\varepsilon_{ef} = \varepsilon_b + \frac{\frac{1}{3}\sum_{i=1}^{n} f_i\left(\varepsilon_i - \varepsilon_b\right)\sum_{k=1}^{3}\frac{\varepsilon_b}{\varepsilon_b + N_{ik}\left(\varepsilon_i - \varepsilon_b\right)}}{1 - \frac{1}{3}\sum_{i=1}^{n} f_i\left(\varepsilon_i - \varepsilon_b\right)\sum_{k=1}^{3}\frac{N_{ik}}{\varepsilon_b + N_{ik}\left(\varepsilon_i - \varepsilon_b\right)}}$$

Here

| | |
|---|---|
| $\varepsilon_b$ | Permittivity of polymer matrix |
| $\varepsilon_i$ | Permittivity of nanofiller inclusions |
| $\varepsilon_{eff}$ | Effective permittivity of nanocomposite |
| $N_{ik}$ | Depolarization factor of the nanofiller inclusions |

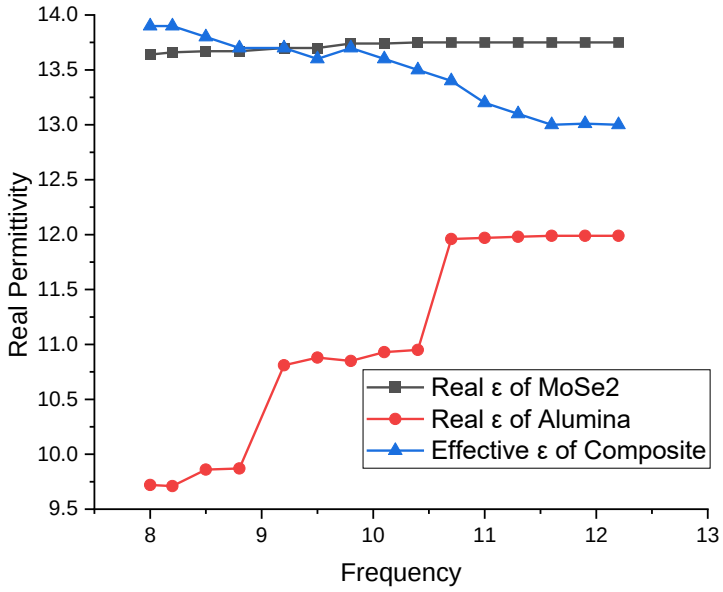


Fig 4.1. Real Permittivity (έ) of $MoSe_2$, Alumina and its Composites

The figure 4.1 illustrates, the change in real permittivity έ values of $MoSe_2$ composite with Alumina. The permittivity values of $MoSe_2$ are above 13.5, and that of Alumina lies 9.3, but after composite formation it falls within a certain range.

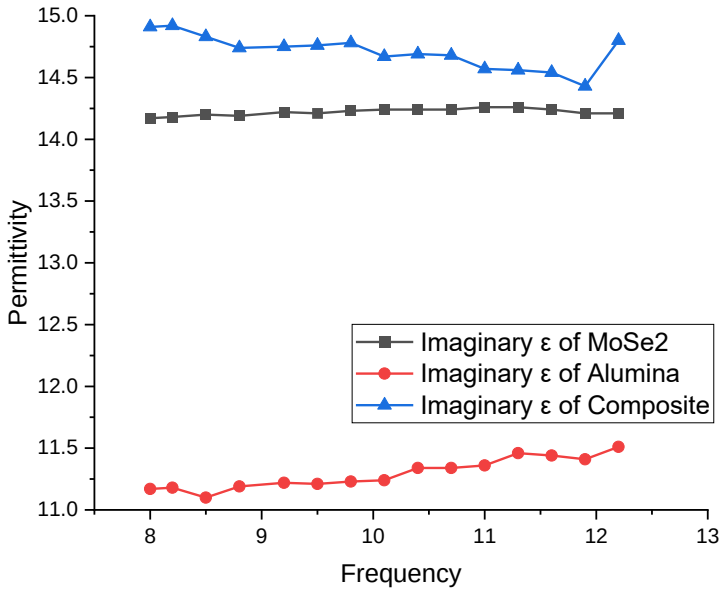


Fig 4.2. Imaginary Permittivity (ε″) of $MoSe_2$ and Alumina and its composite

The effective permittivity value of the composite is enhanced and lies above the $MoSe_2$ as well as alumina. Permittivity varies with location in a medium, frequency of an applied field, humidity, temperature, and other factors.

**Permittivity Tables X - band**

Table 4.1: Real, Imaginary and Effective Permittivity of 0.4% $MoSe_2$ Composite with Alumina in X – Band Region

| S.No | Frequency (GHz) | Real Permittivity ($MoSe_2$) έ | Real Permittivity (Alumina) έ | $\varepsilon_{eff}$ (Effective Real Permittivity of Composite) | Imaginary Permittivity ($MoSe_2$) ε″ | Imaginary Permittivity (Alumina) ε″ | $\varepsilon_{eff}$ (Effective Imaginary Permittivity of Composite) |
|---|---|---|---|---|---|---|---|
| 1 | 8.0 | 13.64 | 9.72 | 13.9 | 14.17 | 11.17 | 14.91 |
| 2 | 8.2 | 13.66 | 9.71 | 13.9 | 14.18 | 11.18 | 14.92 |
| 3 | 8.5 | 13.67 | 9.66 | 13.8 | 14.2 | 11.1 | 14.83 |
| 4 | 8.8 | 13.67 | 9.63 | 13.7 | 14.19 | 11.19 | 14.74 |
| 5 | 9.2 | 13.70 | 10.61 | 13.7 | 14.22 | 11.22 | 14.75 |
| 6 | 9.5 | 13.70 | 10.58 | 13.6 | 14.21 | 11.21 | 14.76 |
| 7 | 9.8 | 13.74 | 10.55 | 13.7 | 14.23 | 11.23 | 14.78 |
| 8 | 10.1 | 13.74 | 10.53 | 13.6 | 14.24 | 11.24 | 14.67 |
| 9 | 10.4 | 13.75 | 10.5 | 13.5 | 14.24 | 11.34 | 14.69 |
| 10 | 10.7 | 13.75 | 11.48 | 13.4 | 14.24 | 11.34 | 14.68 |
| 11 | 11 | 13.75 | 11.46 | 13.2 | 14.26 | 11.36 | 14.57 |
| 12 | 11.3 | 13.75 | 11.43 | 13.1 | 14.26 | 11.46 | 14.56 |
| 13 | 11.6 | 13.75 | 11.41 | 13.0 | 14.24 | 11.44 | 14.54 |
| 14 | 11.9 | 13.75 | 11.49 | 13.9 | 14.21 | 11.41 | 14.43 |
| 15 | 12.2 | 13.75 | 11.46 | 13.8 | 14.21 | 11.51 | 14.41 |

The addition of Alumina in $MoSe_2$ enhanced the effective permittivity values, as is apparent in table 4.1. At 8GHz frequency the real permittivity (έ) for $MoSe_2$ matrix is 13.64 and of Alumina is 9.72, while after composite formation the value is 13.9, which lies above of the two corresponding values. Similarly, the effective imaginary permittivity (ε″) is enhanced after composite formation.At 8GHz the value for the $MoSe_2$/Alumina composite the value is 14.91, which is greater than the effective permittivity value of $MoSe_2$ and Alumina.

Table 4.2: Real, Imaginary and Effective Permittivity of 0.4% $MoSe_2$ Composite with $MoS_2$ in X – Band Region

| S.No | Frequency (GHz) | Real Permittivity ($MoSe_2$) έ | Real Permittivity ($MoS_2$) έ | $\varepsilon_{eff}$ (Effective Real Permittivity of Composite) | Imaginary Permittivity ($MoSe_2$) ε″ | Imaginary Permittivity ($MoS_2$) ε″ | $\varepsilon_{eff}$ (Effective Imaginary Permittivity of Composite) |
|---|---|---|---|---|---|---|---|
| 1 | 8.0 | 13.64 | 29.92 | 14.95 | 14.17 | 14.95 | 15.68 |
| 1 | 8.2 | 13.66 | 29.9 | 14.84 | 14.18 | 14.94 | 15.56 |
| 2 | 8.5 | 13.67 | 29.86 | 14.73 | 14.2 | 14.93 | 15.44 |
| 3 | 8.8 | 13.67 | 29.83 | 14.62 | 14.19 | 14.92 | 15.32 |
| 4 | 9.2 | 13.70 | 29.81 | 14.51 | 14.22 | 14.90 | 15.21 |
| 5 | 9.5 | 13.70 | 29.78 | 14.42 | 14.21 | 14.87 | 15.09 |
| 6 | 9.8 | 13.74 | 29.75 | 14.33 | 14.23 | 14.86 | 15.17 |
| 7 | 10.1 | 13.74 | 29.73 | 14.25 | 14.24 | 14.81 | 15.25 |
| 8 | 10.4 | 13.75 | 29.70 | 14.17 | 14.24 | 14.81 | 15.33 |
| 9 | 10.7 | 13.75 | 29.68 | 14.09 | 14.24 | 14.85 | 15.42 |
| 10 | 11 | 13.75 | 29.66 | 14.21 | 14.26 | 14.79 | 15.51 |
| 11 | 11.3 | 13.75 | 29.63 | 14.32 | 14.26 | 14.78 | 15.62 |
| 12 | 11.6 | 13.75 | 29.61 | 14.44 | 14.24 | 14.78 | 15.73 |
| 13 | 11.9 | 13.75 | 29.59 | 14.56 | 14.21 | 14.76 | 15.84 |
| 14 | 12.2 | 13.75 | 29.56 | 14.68 | 14.21 | 14.64 | 15.95 |

For $MoSe_2/MoS_2$ composite the quantities of effective permittivity are changed. For the 8 GHz the real permittivity value for $MoSe_2$ is 13.64 and 29.92 for $MoS_2$ which changes to 14.95. When compared to the value for $MoS_2$, the real permittivity exhibits significant improvement. Also, the imaginary part is changed as well. AT 8 GHz this value is 13.64 for $MoSe_2$ and for $MoS_2$ is 29.92, while composite value lies in the middle of the two components.

### 4.2 EMI Shielding in Ku – Band Studies:

**Effective Permittivity:**

In Ku band region, the effective permittivity values are modified for all the composites as in X-band region

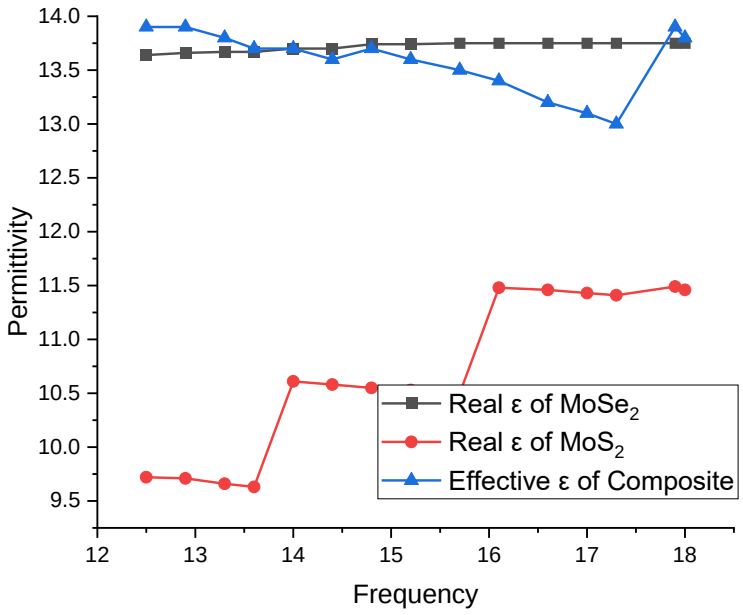


Fig 4.3 Permittivity of $MoSe_2$, $MoS_2$ and $MoSe_2/MoS_2$ Composites

In Molybdenum diselenide composite with Molybdenum disulfide the real permittivity is altered. The value lies between 13.5 to 14.0 (real permittivity value for Molybdenum diselenide), and 11.5 (the maximum real permittivity value for Molybdenum disulfide).

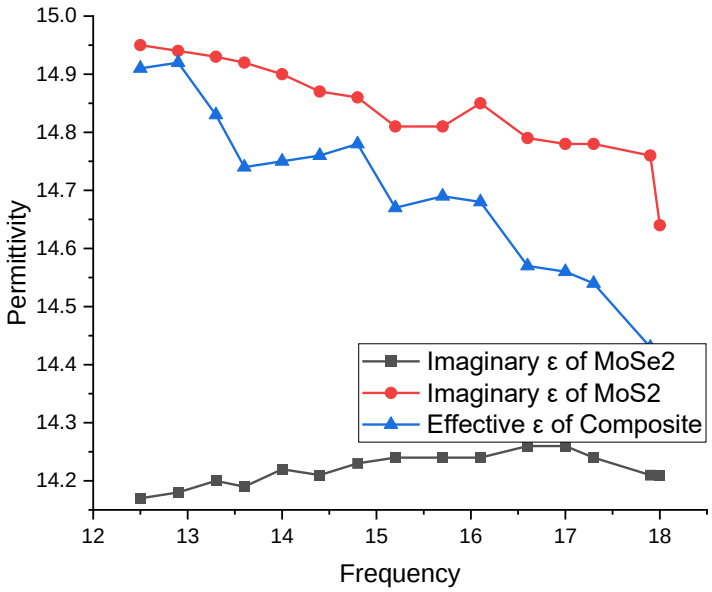


Fig 4.4 Permittivity of MoSe2, MoS2 and MoSe2/MoS2 Composites

The imaginary permittivity part is somehow reduced for nanocomposite when we compared it with imaginary permittivity value of Molybdenum diselenide ($MoSe_2$). Imaginary permittivity ($\varepsilon''$) of Molybdenum diselenide, which is between 14.2 for all frequencies in Ku band range. The polymer matrix serves as the primary component of a nanocomposite, whereas the nanofiller only makes up a minor part of the overall composition.

**Permittivity Tables Ku band**

Table 4.3 : Real and Imaginary Effective Permittivity of 0.4% MoSe2 Composite MoS2

| S.No | Frequency (GHz) | Real Permittivity (MoSe2) έ | Real Permittivity (MoS2) έ | $\varepsilon_{eff}$ (Effective Real Permittivity of Composite) | Imaginary Permittivity(MoSe2) ε″ | Imaginary Permittivity (MoS2) ε″ | $\varepsilon_{eff}$ (Effective Imaginary Permittivity of Composite) |
|---|---|---|---|---|---|---|---|
| 1 | 12.5 | 13.64 | 9.72 | 13.9 | 14.17 | 11.17 | 14.91 |
| 2 | 12.9 | 13.66 | 9.71 | 13.9 | 14.18 | 11.18 | 14.92 |
| 3 | 13.3 | 13.67 | 9.66 | 13.8 | 14.2 | 11.1 | 14.83 |
| 4 | 13.6 | 13.67 | 9.63 | 13.7 | 14.19 | 11.19 | 14.74 |
| 5 | 14.0 | 13.70 | 10.61 | 13.7 | 14.22 | 11.22 | 14.75 |
| 6 | 14.4 | 13.70 | 10.58 | 13.6 | 14.21 | 11.21 | 14.76 |
| 7 | 14.8 | 13.74 | 10.55 | 13.7 | 14.23 | 11.23 | 14.78 |
| 8 | 15.2 | 13.74 | 10.53 | 13.6 | 14.24 | 11.24 | 14.67 |
| 9 | 15.7 | 13.75 | 10.5 | 13.5 | 14.24 | 11.34 | 14.69 |
| 10 | 16.1 | 13.75 | 11.48 | 13.4 | 14.24 | 11.34 | 14.68 |
| 11 | 16.6 | 13.75 | 11.46 | 13.2 | 14.26 | 11.36 | 14.57 |
| 12 | 17.0 | 13.75 | 11.43 | 13.1 | 14.26 | 11.46 | 14.56 |
| 13 | 17.3 | 13.75 | 11.41 | 13.0 | 14.24 | 11.44 | 14.54 |
| 14 | 17.9 | 13.75 | 11.49 | 13.9 | 14.21 | 11.41 | 14.43 |
| 15 | 18 | 13.75 | 11.46 | 13.8 | 14.21 | 11.51 | 14.41 |

The permittivity values for both real (έ) and imaginary ε″) parts are substitute during the formation of nanocomposites, then their pure components, i.e., $MoSe_2$ and $MoS_2$. For example, at 12.5GHz, the έ value for $MoSe_2$ is 13.64 and for $MoS_2$ is 9.72. After composite formation the effective permittivity (εeff) is altered on 13.9. The imaginary part of permittivity reduces too. At 12.5 GHz 14.91 for the composite.

Table 4.4 : Real and Imaginary Effective Permittivity of 0.4% MoSe2 Composites with MoS2

| S.No | Frequency (GHz) | Real Permittivity ($MoSe_2$) έ | Real Permittivity ($MoS_2$) έ | $\varepsilon_{eff}$ (Effective Real Permittivity of Composite) | Imaginary Permittivity ($MoSe_2$) ε″ | Imaginary Permittivity ($MoS_2$) ε″ | $\varepsilon_{eff}$ (Effective Imaginary Permittivity of Composite) |
|---|---|---|---|---|---|---|---|
| 1 | 12.5 | 13.64 | 29.92 | 14.95 | 14.17 | 14.95 | 15.68 |
| 2 | 12.9 | 13.66 | 29.9 | 14.84 | 14.18 | 14.94 | 15.56 |
| 3 | 13.3 | 13.67 | 29.86 | 14.73 | 14.2 | 14.93 | 15.44 |
| 4 | 13.6 | 13.67 | 29.83 | 14.62 | 14.19 | 14.92 | 15.32 |
| 5 | 14.0 | 13.70 | 29.81 | 14.51 | 14.22 | 14.90 | 15.21 |
| 6 | 14.4 | 13.70 | 29.78 | 14.42 | 14.21 | 14.87 | 15.09 |
| 7 | 14.8 | 13.74 | 29.75 | 14.33 | 14.23 | 14.86 | 14.17 |
| 8 | 15.2 | 13.74 | 29.73 | 14.25 | 14.24 | 14.81 | 14.25 |
| 9 | 15.7 | 13.75 | 29.70 | 14.17 | 14.24 | 14.81 | 14.33 |
| 10 | 16.1 | 13.75 | 29.68 | 14.09 | 14.24 | 14.85 | 14.42 |
| 11 | 16.6 | 13.75 | 29.66 | 13.21 | 14.26 | 14.79 | 14.51 |
| 12 | 17.0 | 13.76 | 29.63 | 13.32 | 14.26 | 14.78 | 14.62 |
| 13 | 17.3 | 13.78 | 29.61 | 13.44 | 14.24 | 14.78 | 14.73 |
| 14 | 17.9 | 13.79 | 29.59 | 13.56 | 14.21 | 14.76 | 14.84 |
| 15 | 18 | 13.81 | 29.56 | 13.68 | 14.21 | 14.64 | 14.95 |

The real permittivity (έ) value for $MoSe_2$ composite for $MoS_2$ is altered in the middle of the two values, i.e., for $MoSe_2$ and $MoS_2$. At 12.5GHz this value is 14.95 for nanocomposite, while for $MoSe_2$ it is 13.64, and for $MoS_2$ it is 29.92. Similarly, at this frequency i.e., 12.9GHz, the imaginary permittivity of nanocomposite is 15.56, while it is 14.17 for $MoSe_2$ and 14.95 for MoS

### 4.3 EMI Shielding Effectiveness in X_Band and Ku_Band range

### $MoSe_2$/Alumina Composite

There are three types of losses that can occur during electromagnetic shielding reflection loss, absorption loss and multiple internal reflections. To name a few: reflection , absorption and multiple reflection loss. Our research shows that for all two composites, the key factor in the shielding effect depends on the Reflection mechanism in X_band range, therefore the Reflection Loss ($R_L$) tells us how well the composite dampens the microwaves.

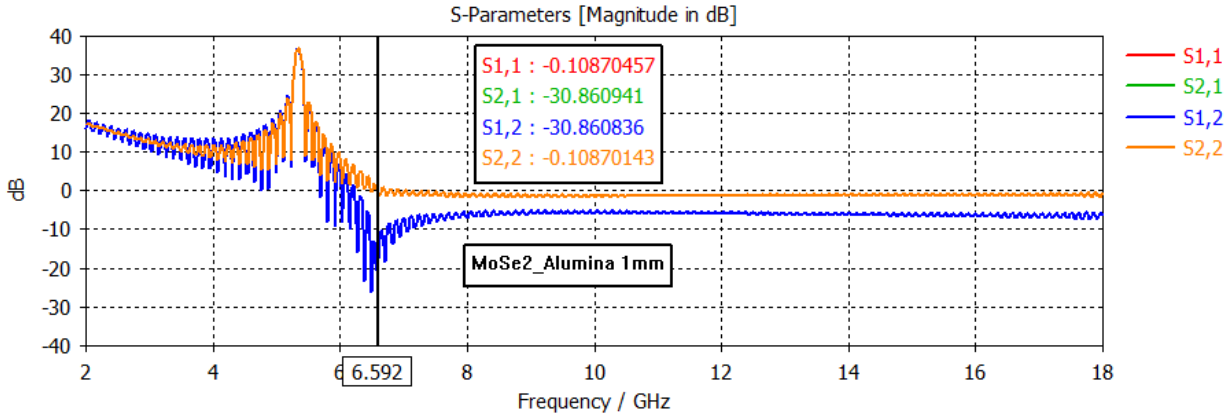


Fig 4.5. RL value for $MoSe_2$/Alumina Composite with 1mm thickness

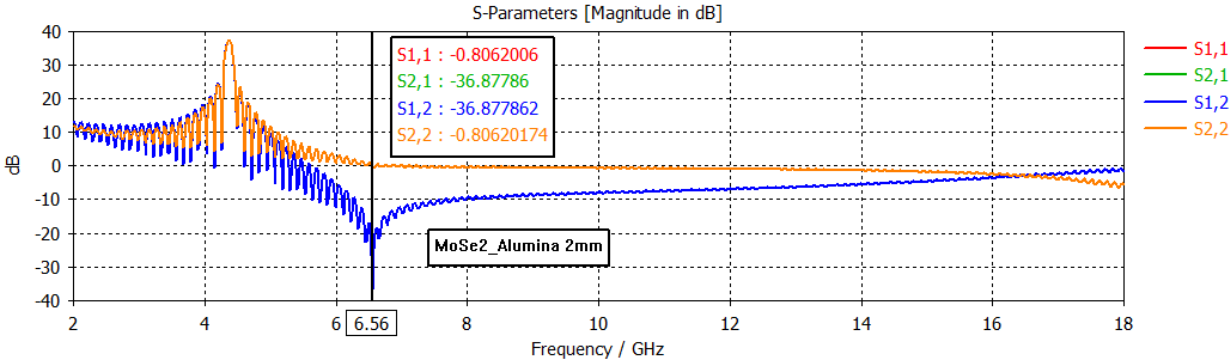


Fig 4.6. RL value for $MoSe_2$/Alumina Composite with 2mm thickness

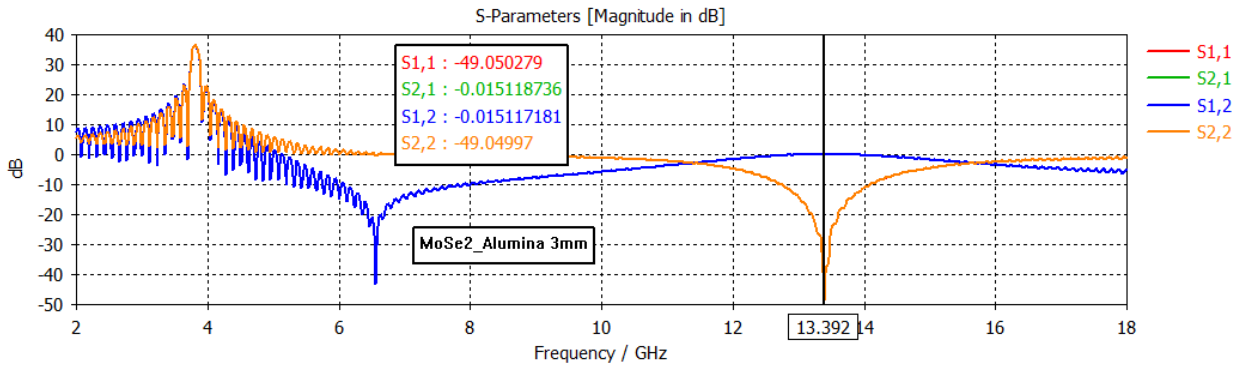


Fig 4.7. RL value for $MoSe_2$/Alumina Composite with 3mm thickness

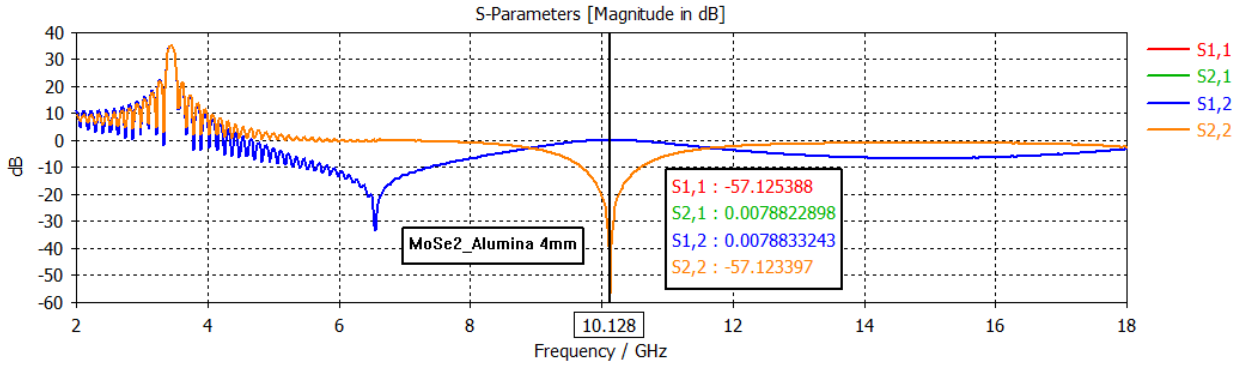


Fig 4.8. RL value for $MoSe_2$/Alumina Composite with 4mm thickness

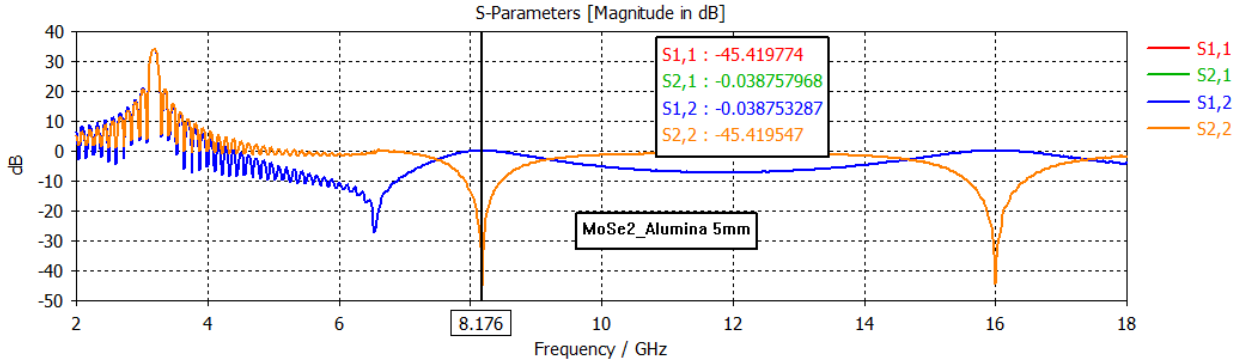


Fig 4.9. RL value for $MoSe_2$/Alumina Composite with 5mm thickness

### $MoSe_2/MoS_2$ Composite

In the case of the Ku band, each of the four composites implements the reflection mechanism for the purpose of electromagnetic shielding. The following figures illustrate the reflection loss shown by different composites in thicknesses ranging from 1 to 5 millimeters.

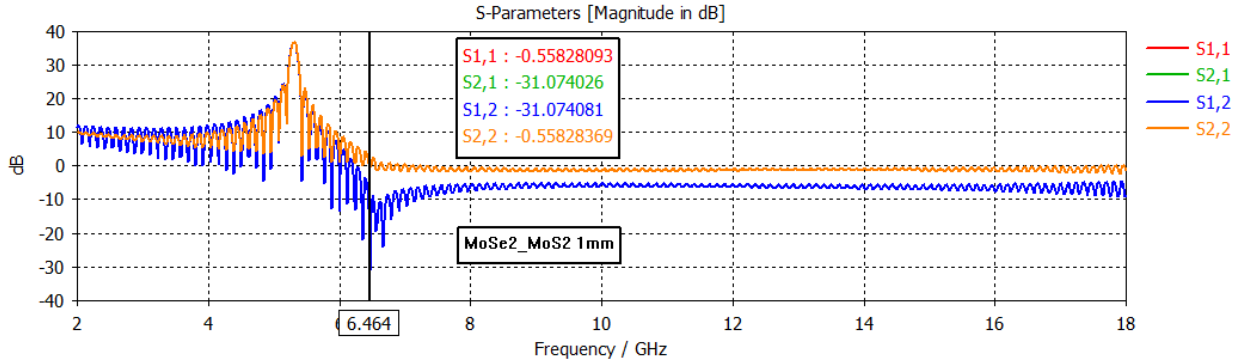


Fig 4.10. Real Permittivity of $MoSe_2$, $MoS_2$ and $MoSe_2/MoS_2$ Composites for 1mm

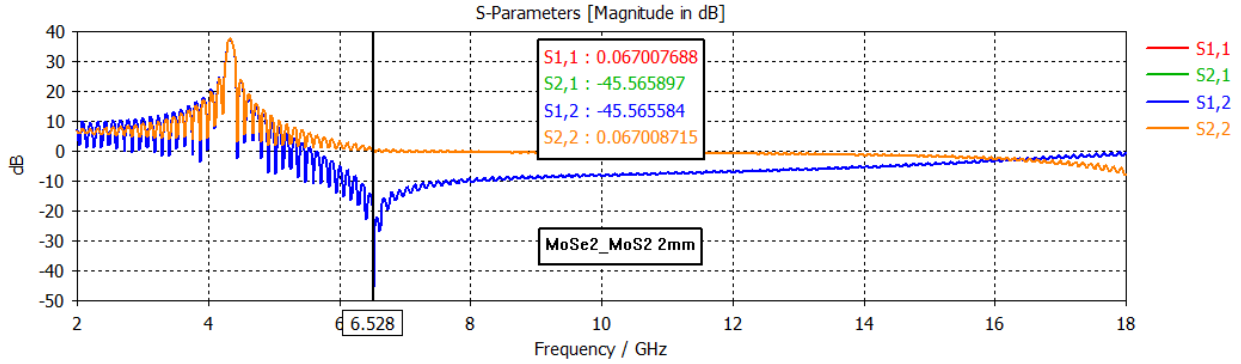


Fig 4.11. Real Permittivity of $MoSe_2$, $MoS_2$ and $MoSe_2/MoS_2$ Composites for 2mm

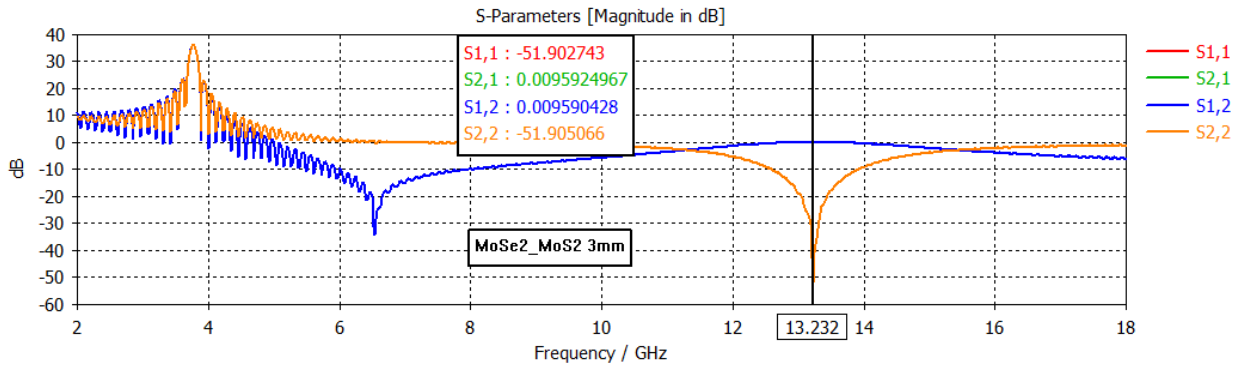


Fig 4.12. Real Permittivity of $MoSe_2$, $MoS_2$ and $MoSe_2/MoS_2$ Composites for 3mm

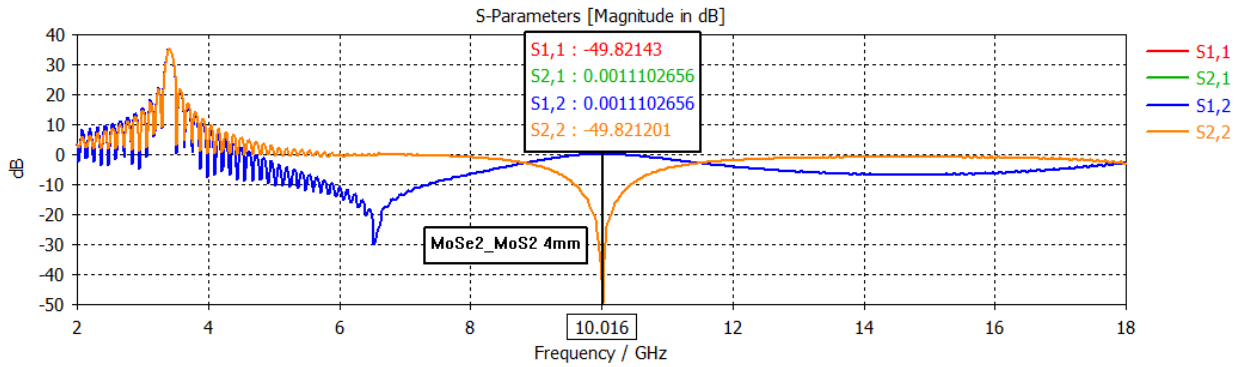


Fig 4.13. Real Permittivity of $MoSe_2$, $MoS_2$ and $MoSe_2/MoS_2$ Composites

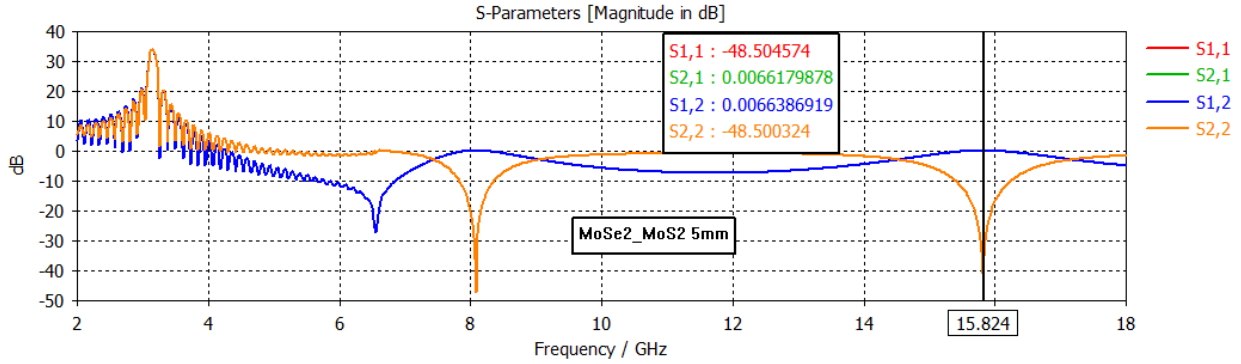


Fig 4.14. Real Permittivity of $MoSe_2$, $MoS_2$ and $MoSe_2/MoS_2$ Composites

### 4.4 Comparison between $MoSe_2$/Alumina and $MoSe_2/MoS_2$ Composites:

For making a comparison, we have only chosen values of reflection loss for the samples that produced the highest in the X_band and Ku_band range for microwave spectrum.

### $MoSe_2$ Composites with $MoS_2$

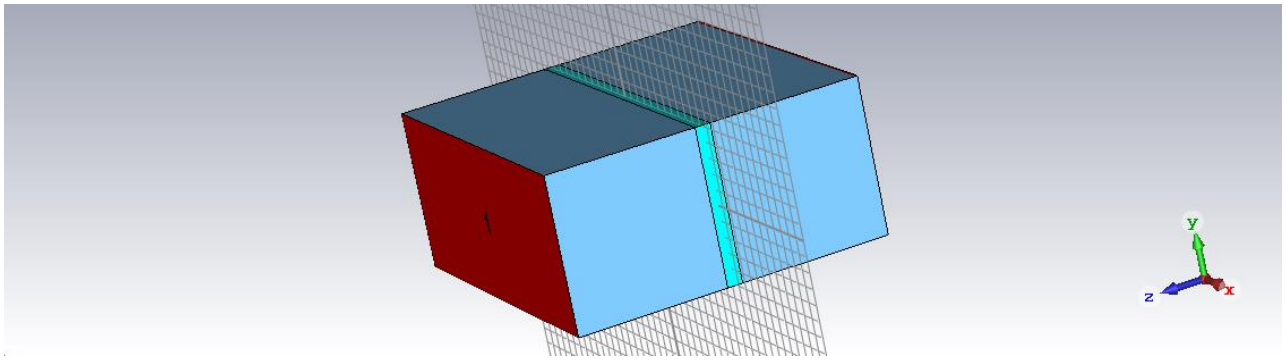

Fig 4.15. 1mm Thick MoSe2 with Alumina in CST Studio Waveguide Model

Five samples, ranging in thickness from 1mm to 5mm, have been simulated. Samples of each composite are being compared at different thicknesses because these values indicate less reflection loss at these sizes from 1mm to 2mm. In the 10GHz area, the MoSe2 bundles 4mm sample had the maximum reflection loss value of -57.12dB, while composite having 3mm thickness offered the highest reflection loss value of -49.05dB at 13GHz.

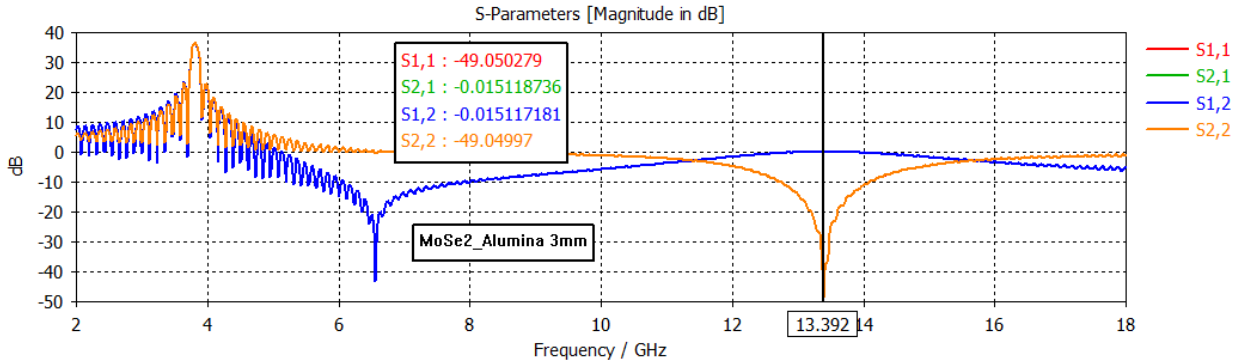


Fig 4.16: RL Values for MoSe2/Alumina composite for 3mm thickness

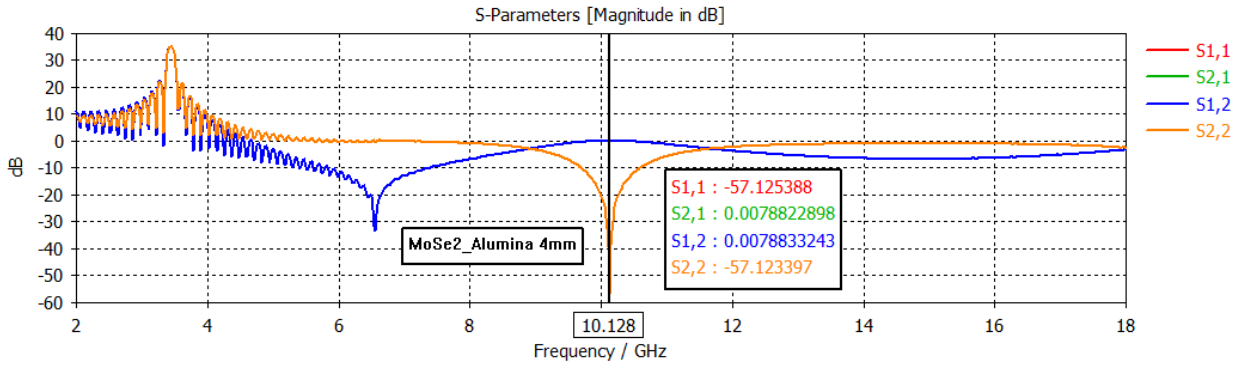


Fig 4.17. RL Values for MoSe2/Alumina composite for 4mm thickness.

# Chapter 5: Conclusion

Multiple samples of MoSe2 composites having varying thicknesses (1mm-5mm) were tested for Ku_band 12-18GHz X_band 8-12GHz rates by using methods like frequency difference time domain (FDTD), to perform high frequency simulation tasks. The results indicated that the composites performed exceptionally well in both frequency ranges, particularly for samples with thicknesses of 3mm and 4mm.

A 3mm sample of the MoSe2/MoS2 composite showed a reflection loss value of -51.90dB at a 13GHz frequency, laying in the Ku-band region. The same composite with a thickness of 4mm, exhibited slightly lower reflection loss value -49.82dB at 10GHz compared to the 3mm thick sample. Material was particularly noteworthy due to its good reflection loss value and better heat dissipation, making it potentially useful in various applications.

For MoSe2/Alumina composite, sample 4mm thickness exhibited -57.12dB reflection loss value at 10GHz frequency range in the X-band region. Same composite with 3mm thick sample showed -49.05dB reflection loss value at 13GHz frequency range indicating that results are efficient in both X-band and the Ku-band.

With the help of the findings, designed composite materials can exhibit great utility in plenty of fields, such as the electronic gadgets and for the defense industry due to their high absorption tendencies of microwaves radiation even at low thickness. Computational investigations revealed that the designed composites can be effectively employed as coating material, however experimental testing is required for the validation of computational findings.

**Future Perspective**

MAMs have been found useful in various contexts, but they have been particularly beneficial in satellite communication. A recent study has represented a significant advancement in this area as it has enabled the creation of nanocomposites using effective medium theories by knowing the permittivity values of the matrix and the nanofiller. A computer model of a waveguide was developed in the study, which has enabled the determination of the microwave absorption behavior of practically any material between 8 and 18 GHz. By predicting the microwave absorption tendency using a computational model, the data can be utilized to synthesize and construct improved MAMs in the future.

## References:


1. Green, M. & Chen, X. Recent progress of nanomaterials for microwave absorption. Journal of Materiomics vol. 5 503–541 (2019).
2. Stock, N. & Biswas, S. Synthesis of metal-organic frameworks (MOFs): Routes to various MOF topologies, morphologies, and composites. Chemical Reviews vol. 112 933–969 (2012).
3. Chen, L., Lan, C., Xu, B. & Bi, K. Progress on material characterization methods under big data environment. Advanced Composites and Hybrid Materials vol. 4 235–247 (2021).
4. Kumar, A., Agarwala, V. & Singh, D. Effect of milling on dielectric and microwave absorption properties of SiC based composites. Ceram Int 40, 1797–1806 (2014).
5. Qi, X. *et al*. Metal-free carbon nanotubes: Synthesis, and enhanced intrinsic microwave absorption properties. Sci Rep 6, (2016).
6. Müller, K. *et al*. Review on the processing and properties of polymer nanocomposites and nanocoatings and their applications in the packaging, automotive and solar energy fields. Nanomaterials vol. 7 (2017).
7. Fu, Y. C. Microwave heating in food processing. in Handbook of Food Science, Technology, and Engineering - 4 Volume Set 2258–2272 (CRC Press, 2005).
8. Zhao, L. *et al*. Relationship between cognition function and hippocampus structure after long-term microwave exposure. Biomedical and Environmental Sciences 25, 182–188 (2012).
9. Saveleva, M. S. *et al*. Hierarchy of hybrid materials-the place of inorganics-in-organics in it, their composition, and applications. Frontiers in Chemistry vol. 7 (2019).
10. Zamorano Ulloa, R., Guadalupe Hernandez Santiago, Ma. & L. Villegas Rueda, V. The Interaction of Microwaves with Materials of Different Properties in Electromagnetic Fields and Waves (IntechOpen, 2019).
11. Rohini, R. & Bose, S. Electromagnetic wave suppressors derived from crosslinked polymer composites containing functional particles: Potential and key challenges. Nanostructures and Nano-Objects vol. 12 130–146 (2017).
12. Jiang, D. *et al*. Electromagnetic Interference Shielding Polymers and Nanocomposites - A Review. Polymer Reviews vol. 59 280–337 (2019).
13. Al-Jumaily, A. H. J., Sali, A., Mandeep, J. S. & Ismail, A. Propagation measurement on earth-sky signal effects for high-speed train satellite channel in tropical region at Ku-band. Int. J. Antennas Propag. (2015).
14. Zhu, X. assessing effective medium theories for designing composites for nonlinear transmission lines. (2019).
15. Folgueras, L. de C., Alves, M. A. & Rezende, M. C. Microwave absorbing paints and sheets based on carbonyl iron and polyaniline: Measurement and simulation of their properties. Journal of Aerospace Technology and Management 2, 63–70 (2010).

16. Younes, H. *et al*. thin carbon nanostructure mat with high electromagnetic interference shielding performance. Synth. Met. 253, 48–56 (2019).

17. Munalli, D., Dimitrakis, G., Chronopoulos, D., Greedy, S. & Long, A. Electromagnetic shielding effectiveness of carbon fibre reinforced composites.

18. Hong, W., Xiao, P., Luo, H. & Li, Z. Microwave axial dielectric properties of carbon fiber. Sci Rep 5, (2015).

19. Chen, L., Wang, H. F., Li, C. & Xu, Q. Bimetallic metal-organic frameworks, and their derivatives. Chemical Science vol. 11 5369–5403 (2020).

20. Lv, H., Ji, G., Liang, X. H., Zhang, H. & Du, Y. A novel rod-like MnO2/Fe loading on graphene giving excellent electromagnetic absorption properties. J Mater Chem C Mater 3, 5056–5064 (2015).

21. He, G., Duan, Y., Pang, H. & Zhang, X. Rational design of mesoporous MnO2 microwave absorber with tunable microwave frequency response. Appl Surf Sci 490, 372–382 (2019).

22. Che, B. D. *et al*. The impact of different multi-walled carbon nanotubes on the X-band microwave absorption of their epoxy nanocomposites. Chem Cent J 9, (2015).

23. Savi, P., Giorcelli, M. & Quaranta, S. Multi-walled carbon nanotubes composites for microwave absorbing applications. Applied Sciences 9, (2019).

24. Wang, Y. *et al*. Enhanced microwave absorption properties of MnO2 hollow microspheres consisted of MnO2 nanoribbons synthesized by a facile hydrothermal method. J Alloys Compd 676, 224–230 (2016).

25. Bora, P. J., Vinoy, K. J., Ramamurthy, P. C. & Madras, G. Electromagnetic interference shielding efficiency of MnO2 nanorod doped polyaniline film. Mater Res Express 4, (2017).

26. Zhu, X. assessing effective medium theories for designing composites for nonlinear transmission lines. (2019).

27. Folgueras, L. de C., Alves, M. A. & Rezende, M. C. Microwave absorbing paints and sheets based on carbonyl iron and polyaniline: Measurement and simulation of their properties. Journal of Aerospace Technology and Management 2, 63–70 (2010).

28. Guo, M., Jiang, X. & Fu, H. Preparation and Study of Novel Modified [(1-x) MnO2-xMWCNTs]/Waterborne Polyurethane Composites with Microwave Absorption Properties. Ind Eng Chem Res 57, 13406–13416 (2018).

29. Singh, S., Kumar, A. & Singh, D. Enhanced Microwave Absorption Performance of SWCNT/SiC Composites. J Electron Mater 49, 7279–7291 (2020).

30. Wang, C. *et al*. The electromagnetic property of chemically reduced graphene oxide and its application as microwave absorbing material. Appl Phys Lett 98, (2011).

31. Hussein, M. I. *et al*. Microwave Absorbing properties of metal functionalized-CNT-polymer composite for stealth applications. Sci Rep 10, (2020).

32. Wang, C. *et al*. The electromagnetic property of chemically reduced graphene oxide and its application as microwave absorbing material. Appl Phys Lett 98, (2011).

33. Green, M. *et al*. Ferric metal-organic framework for microwave absorption. Mater Today Chem 9, 140–148 (2018).

34. Nowotny, M. K., Bak, T. & Nowotny, J. Electrical properties and defect chemistry of TiO2 single crystal. II. Thermoelectric power. Journal of Physical Chemistry B 110, 16283–16291 (2006).

35. Zhang, D. *et al*. An electromagnetic wave absorbing material with potential application prospects—WS2 nanosheets. Integrated Ferroelectrics 200, 108–116 (2019).

36. Chu, Z., Cheng, H., Xie, W. & Sun, L. Effects of diameter and hollow structure on the microwave absorption properties of short carbon fibers. Ceram. Int. 38, 4867–4873 (2012).

37. Said, R. A. M., Hasan, M. A., Abdelzaher, A. M. & Abdel-Raoof, A. M. Review—Insights into the Developments of Nanocomposites for Its Processing and Application as Sensing Materials. J Electrochem Soc 167, 037549 (2020).

38. Singh, S. & Kapoor, N. Health Implications of Electromagnetic Fields, Mechanisms of Action, and Research Needs. Adv. Biol. 2014, 1–24 (2014).

39. Al-Ghamdi, A. A., Al-Hartomy, O. A., Al-Solamy, F., Al-Ghamdi, A. A. & El-Tantawy, F. Electromagnetic wave shielding and microwave absorbing properties of hybrid epoxy resin/foliated graphite nanocomposites. J. Appl. Polym. Sci. 127, 2227–2234 (2013).

40. Galeev, A. L. The Effects of Microwave Radiation from Mobile Telephones on Humans and Animals. Rossiiskii Fiziologicheskii Zhurnal imeni L. M. Sechenova vol. 30 (2000).

41. Delhi, N. & Behari, J. Electromagnetic pollution - The causes and concerns. in Proceedings of the International Conference on Electromagnetic Interference and Compatibility vols 316–320 Institute of Electrical and Electronics Engineers Inc., (2002).

42. Kreyling, W. G., Semmler-Behnke, M. & Chaudhry, Q. A complementary definition of nanomaterial. Nano. Today 5, 165–168 (2010).

43. Skolnik, M. Role of radar in microwaves. IEEE Trans Microw Theory Tech. 50, 625–632 (2002).

44. Hao, Y. H., Zhao, L. & Peng, R. Y. Effects of microwave radiation on brain energy metabolism and related mechanisms. Military Medical Research vol. 2 (2015).

45. Deniz, O. *et al*. Effects of short and long-term electromagnetic fields exposure on the human hippocampus. J. Microsc. Ultrastruct. 5, 191 (2017).

46. Heynick, L. N., Johnston, S. A. & Mason, P. A. Radio Frequency Electromagnetic Fields: Cancer, Mutagenesis, and Genotoxicity in Bioelectromagnetics vol. 24 (2003).

47. Shahin, S. *et al*. 2.45 GHz microwave irradiation-induced oxidative stress affects implantation or pregnancy in mice, musculus. Appl. Biochem. Biotechnol. 169, 1727–1751 (2013).

48. Panias, D., Krestou, A., Panias, D. & Krestou, A. Use of Microwave Energy in Metallurgy Mineralogy and distribution of the secondary and trace bauxite elements through the Bayer process and its by-products View project Eurare View project Use of Microwave energy in Metallurgy. https://www.researchgate.net/publication/234107697 (2004).

49. Özkaya, U., 2+, S. & Yaldız, E. Analysis of Electromagnetic Radiation in Daily Life. SETSCI Conference Indexing System vol. 3 (2018).

50. Zhi, W. J., Wang, L. F. & Hu, X. J. Recent advances in the effects of microwave radiation on brains. Military Medical Research vol. 4 (2017).

51. Memon, D. H. The Future of Satellite Communications in Pakistan. CCIS vol. 20 (2008).

52. Lewicka, M. *et al*. The effect of electromagnetic radiation emitted by display screens on cell oxygen metabolism-in vitro studies. Archives of Medical Science 11, 1330–1339 (2015).

53. Li, Z., Haigh, A., Soutis, C., Gibson, A. & Sloan, R. A Simulation-Assisted Non-destructive Approach for Permittivity Measurement Using an Open-Ended Microwave Waveguide. J Nondestr Eval 37, (2018).

54. Azizi-Lalabadi, M., Hashemi, H., Feng, J. & Jafari, S. M. Carbon nanomaterials against pathogens; the antimicrobial activity of carbon nanotubes, graphene/graphene oxide, fullerenes, and their nanocomposites. Advances in Colloid and Interface Science vol. 284 (2020).

55. Green, M. & Chen, X. Recent progress of nanomaterials for microwave absorption. Journal of Materiomics vol. 5 503–541 (2019).

56. Muhamad, M. I., Seroji, M. N., IEEE Malaysia Section, IEEE Power & Energy Society. Malaysia Chapter & Institute of Electrical and Electronics Engineers. 2014 IEEE International Conference on Power and Energy (PECon) : conference proceeding : Dec 1st-3rd, 2014, Pullman Hotel, Kuching, Sarawak, Malaysia.

57. Yakovenko, O. S. *et al*. Complex permittivity of polymer-based composites with carbon nanotubes in microwave band. Applied Nanoscience 10, 2691–2697 (2020).

58. Matitsine, S. M. *et al.* Shift of resonance frequency of long conducting fibers embedded in a composite. J Appl Phys 94, 1146–1154 (2003).

59. Koledintseva, M. Y., Dubroff, R. E. & Schwartz, R. W. Maxwell Garnett model for dielectric mixtures containing conducting particles at optical frequencies (postprint) materials and manufacturing directorate air force research laboratory air force Materiel command wright-patterson air force base OH 45433-7750. (2006).

60. Karger-Kocsis, J. (József) & Karger-Kocsis, J. Polypropylene: an A-Z reference. (Kluwer Academic Publishers, 1998).

61. Koledintseva, M. Y., Drewniak, J., Dubroff, R., Rozanov, K. & Archambeault, B. modeling of shielding composite materials and structures for microwave frequencies. Progress In Electromagnetics Research B vol. 15.

62. Loya, S. Analysis of Shielding Effectiveness in the Electric Field and Magnetic Field and Plane Wave for Infinite Sheet Metals. International Journal of Electromagnetics and Applications 6, 31–41 (2016).

63. Li, Z., Wang, Z., Lu, W. & Hou, B. Theoretical study of electromagnetic interference shielding of 2D MXenes films. Metals (Basel) 8, (2018).

64. Li, S. *et al.* Applying effective medium theory in characterizing dielectric constant of solids. in Proceedings of the 2012 International Workshop on Metamaterials, Meta 2012 (2012).

65. Hall, G. Maxwell's electromagnetic theory and special relativity. Philosophical Transactions of the Royal Society A: Mathematical, Physical and Engineering Sciences 366, 1849–1860 (2008).

66. Tinsley, D. M. & Sharp, J. H. thermal analysis of manganese dioxide in controlled atmosphere. Journal of Thermal Analysis vol. 3 (1971).

67. Wang, Z. & Zhao, G.-L. Microwave Absorption Properties of Carbon Nanotubes-Epoxy Composites in a Frequency Range of 2 - 20 GHz. Open Journal of Composite Materials 03, 17–23 (2013).

68. Liew, K. M., Wong, C. H., He, X. Q. & Tan, M. J. Thermal stability of single and multi-walled carbon nanotubes. Phys Rev B Condens Matter Mater Phys 71, (2005).

69. Kučerová, Z. *et al.* Mechanical and microwave absorbing properties of carbon-filled polyurethane. Micron 40, 70–73 (2009).

70. Koledintseva, M. Y., Drewniak, J., Dubroff, R., Rozanov, K. & Archambeault, B. modeling and shielding composite materials and structures for microwave frequencies. Progress In Electromagnetics Research B vol. 15.

71. Decrossas, E., El Sabbagh, M. A., Hanna, V. F. & El-Ghazaly, S. M. Rigorous characterization of carbon nanotube complex permittivity over a broadband of RF frequencies. IEEE Trans Electromagn Compat 54, 81–87 (2012).